Published in final edited form as:

FASEB J. 2022 July ; 36(7): e22400. doi:10.1096/fj.202101956RR.

The role of endogenous Smad7 in regulating macrophage phenotype following myocardial infarction

Jun Li[1,2],

Ruoshui Li[1],

Izabela Tuleta[1],

Silvia C Hernandez[1],

Claudio Humeres[1],

Anis Hanna[1],

Bijun Chen[1],

Nikolaos G Frangogiannis[1]

[1]The Wilf Family Cardiovascular Research Institute, Department of Medicine (Cardiology), Albert Einstein College of Medicine, Bronx NY 10461 USA

[2]Department of Physiology and Pathophysiology, School of Basic Medicine, Fourth Military Medical University, Xi'an, 710032, China

Abstract

Smad7 restrains TGF-β responses, and has been suggested to exert both pro- and anti-inflammatory actions that may involve effects on macrophages. Myocardial infarction triggers a macrophage-driven inflammatory response that plays a central role in cardiac repair, but also contributes to adverse remodeling and fibrosis. We hypothesized that macrophage Smad7 expression may regulate inflammation and fibrosis in the infarcted heart through suppression of TGF-β responses, or via TGF-independent actions. In a mouse model of myocardial infarction, infiltration with Smad7+ macrophages peaked 7 days after coronary occlusion. Myeloid cell-specific Smad7 loss in mice had no effects on homeostatic functions and did not affect baseline macrophage gene expression. RNA-seq predicted that Smad7 may promote TREM1-mediated inflammation in infarct macrophages. However, these alterations in the transcriptional profile of macrophages were associated with a modest and transient reduction in infarct myofibroblast infiltration, and did not affect dysfunction, chamber dilation, scar remodeling, collagen deposition, and macrophage recruitment. In vitro, RNA-seq and PCR arrays showed that TGF-β has profound effects on macrophage profile, attenuating pro-inflammatory cytokine/chemokine expression, modulating synthesis of matrix remodeling genes, inducing genes associated with sphingosine-1 phosphate activating and integrin signaling, and inhibiting cholesterol biosynthesis

Address for correspondence: Nikolaos G Frangogiannis, MD, The Wilf Family Cardiovascular Research Institute, Albert Einstein College of Medicine, 1300 Morris Park Avenue Forchheimer G46B, Bronx NY 10461, Tel: 718-430-3546, Fax: 718-430-8989, nikolaos.frangogiannis@einsteinmed.edu.

AUTHOR CONTRIBUTIONS: J.L and N.G.F performed study concept and design, J.L. R.L., I.T., C.H., A.H., S.C.H. and B.C. performed the experiments, J.L., R.L., I.T, C.H., A.H., S.C.H., B.C, and N.G.F. analyzed and interpreted the data, J.L. and N.G.F. wrote the manuscript, all authors critically revised the manuscript and approved the final version.

CONFLICT OF INTEREST: There are no conflicts to disclose.

genes. However, Smad7 loss did not significantly affect TGF-β-mediated macrophage responses, modulating synthesis of only a small fraction of TGF-β-induced genes, including *Itga5*, *Olfml3* and *Fabp7*. Our findings suggest a limited role for macrophage Smad7 in regulation of post-infarction inflammation and repair, and demonstrate that the anti-inflammatory effects of TGF-β in macrophages are not restrained by endogenous Smad7 induction.

Keywords

macrophage; TGF-β; myocardial infarction; inflammation; fibrosis

INTRODUCTION

Macrophages are critically involved in repair, remodeling and fibrosis of the infarcted heart[1,2]. Following myocardial infarction, the resident cardiac macrophage population[3] is replaced by a large and dynamic population of macrophages, derived from circulating monocytes released by the bone marrow and the spleen[4,5,6,7]. In the healing infarct, macrophages undergo phenotypic changes and contribute to cellular responses critical for repair[8], but also participate in maladaptive processes, promoting fibrosis of the non-infarcted myocardium and accentuating adverse remodeling and myocardial dysfunction[9,10,11]. The contribution of infarct macrophages is prominent in all phases of cardiac repair. During the inflammatory phase, macrophages stimulate the inflammatory cascade[12,13] and phagocytose dead cells and matrix debris[14,6]. Upon phagocytosis of apoptotic cells, macrophages acquire an anti-inflammatory phenotype restraining post-infarction inflammation[15]. During the proliferative phase of healing, macrophage subpopulations activate fibroblasts[16,17] and may promote angiogenesis[18,19]. In the remodeling non-infarcted myocardium, mechanical stress may activate macrophages and can contribute to adverse fibrotic remodeling and dysfunction[10,20].

The members of the TGF-β superfamily potently modulate myeloid cell phenotype and function[21,22]. In the healing infarct, all 3 TGF-β isoforms are induced and activated, and have been suggested to regulate inflammation, repair, remodeling and fibrosis[23,24]. The effects of TGF-βs on mononuclear phagocytes are dependent on the state of differentiation of the cells. In monocytes, TGF-βs exert chemotactic and pro-inflammatory actions, inducing cytokine secretion[25,26], and stimulating integrin synthesis and collagenase expression[27]. In contrast, in macrophages, the effects of TGF-βs are predominantly anti-inflammatory [28,29,30]. Canonical TGF-β signaling is mediated through a series of intracellular effectors, the receptor-activated Smads (R-Smads). Tight regulation of TGF-β/R-Smad signaling is critical to prevent persistent or excessive actions of the cytokine. The inhibitory Smads (I-Smads), Smad6 and Smad7 play an important role in negative regulation of the TGF-β cascade. Smad7 is induced in many different cell types upon stimulation with TGF-β superfamily members, and serves as a negative feedback loop that inhibits TGF-β/R-Smad responses through interactions with the TGF-β receptors, or through disruption of R-Smad activation[31]. Moreover, a growing body of evidence suggests that Smad7 may also have TGF-β independent actions[32].

The role of Smad7 in immune cells is controversial, as experimental studies have produced conflicting results. It has been suggested that Smad7 mediates the anti-inflammatory effects of TGF-β, by binding to the adaptors TAB2 and TAB3, and by inhibiting TAK1 recruitment to TRAF2[33], thus blocking pro-inflammatory TNF signaling, and attenuating NF-κB activation [34]. Other studies have suggested that Smad7 may promote inflammation, by rendering immune cells unresponsive to the anti-inflammatory actions of TGF-β [35,36]. To directly address this controversy, we developed mice with myeloid cell-specific Smad7 loss (MyS7KO mice), and we studied the role of Smad7 in regulation of macrophage phenotype and function following myocardial infarction. Our findings show that Smad7 is induced in a subset of infarct macrophages. RNA-sequencing showed that Smad7 loss did not affect the transcriptomic profile of control macrophages, but had a major impact on gene expression in infarct macrophages. Bioinformatic analysis predicted that Smad7 deletion in infarct macrophages may inhibit the triggering receptor expressed in myeloid cells (TREM)1 pathway and enhance semaphorin signaling, thus attenuating their pro-inflammatory properties. These effects were associated with a modest and transient, but significant reduction in myofibroblast infiltration in MyS7KO infarcts. However, these transcriptomic and cellular alterations did not have a significant impact on post-infarction dysfunction, inflammatory cell infiltration, repair, and adverse remodeling. In vitro, Smad7 loss had minor modulatory effects on the macrophage transcriptome, accentuating synthesis of a small fraction of TGF-β-induced genes, such as *Itga5*, *Fabp7* and *Olfml3*, but without affecting the anti-inflammatory effects of TGF-β on cytokine-stimulated macrophages.

MATERIALS AND METHODS:

Generation of mice with myeloid cell-specific loss of Smad7:

In order to study the role of Smad7 in myeloid cells in vivo, we generated mice with loss of Smad7 in lysozyme M (LyzM)+ cells (MyS7KO). We used a transgenic mouse line in which Cre recombinase is driven by the LyzM promoter (Jackson Laboratory, stock No: 004781). LyzM-Cre mice were bred with Smad7fl/fl mice[37] (Jackson Laboratory, stock No: 017008) to generate LyzM-Cre;Smad7fl/fl animals (MyS7KO) and corresponding Smad7fl/fl control littermates. In order to study the time course of Smad7 activation in macrophages, we used the “MacGreen” $CSF1R^{EGFP}$ reporter mice[38]. These transgenic mice (Jackson Laboratory, stock No: 018549) express enhanced green fluorescent protein (EGFP), under the control of the mouse *Csf1r* proximal promoter. Both male and female mice underwent non-reperfused myocardial infarction protocols.

Generation of mice with global inducible Smad7 loss:

Smad7 KO macrophages were harvested from inducible global Smad7 KO mice. To generate these animals, mice expressing a tamoxifen-inducible, Cre-mediated recombination system driven by the CMV-enhanced global actin promoter (CAGGCre-ER, Jackson Laboratory, stock No: 004682)[39] were crossed for two generations with homozygous Smad7 fl/fl mice [37] (Jackson Laboratory, stock No: 017008) in which the promoter region and exon 1 of *Smad7* are flanked by loxp sites. The mice generated ($CAGGCre^{+/-}$;$Smad7^{fl/fl}$) were injected intraperitoneally at the age of 6 weeks with tamoxifen (100 mg/kg body weight, Sigma-Aldrich #T5648) daily for 5 consecutive days to generate Smad7 global KO animals.

CAGGCre$^{-/-}$;Smad7$^{fl/fl}$ littermates receiving the same tamoxifen injection protocols were used as controls. Smad7 global KO mice and corresponding controls were sacrificed 2 weeks after tamoxifen injection, in order to isolate bone marrow macrophages (BMM). (CAGGCre$^{+/-}$ Smad7$^{fl/fl}$: n=6, 3 males and 3 females. CAGGCre$^{-/-}$ Smad7$^{fl/fl}$: n= 8, 5 males and 3 females). Deletion of Smad7 was confirmed by qPCR and western blotting.

Mouse model of non-reperfused myocardial infarction:

Animal studies were approved by the Institutional Animal Care and Use Committee at Albert Einstein College of Medicine and conform with the Guide for the Care and Use of Laboratory Animals published by the National Institutes of Health. A model of non-reperfused myocardial infarction was induced by permanent ligation of left anterior descending coronary artery, as previously described by our group[15]. MyS7KO mice, Smad7fl/fl littermates, and CSF1R^{EGFP} mice underwent infarction protocols. 3-4 month-old male and female mice were anesthetized using inhaled isoflurane (3% for induction, 2% for maintenance). Intraoperatively, heart rate, respiratory rate and electrocardiogram were continuously monitored, and the depth of anesthesia was assessed using the toe pinch method. The left anterior descending coronary artery was occluded for 24 hours, 3 days, 7 days, 28 days, or 56 days. To assess cardiac function and remodeling following myocardial infarction, animals underwent echocardiographic analysis at baseline and after 7, 28 and 56 days of myocardial infarction. At the end of the experiment, euthanasia was performed using 2% inhaled isoflurane followed by cervical dislocation. Early euthanasia was performed with the following criteria, indicating suffering of the animal: weight loss>20%, vocalization, dehiscent wound, hypothermia, clinical signs of heart failure (cyanosis, dyspnea, tachypnea), lack of movement, hunched back, ruffled coat, lack of food or water ingestion.

Echocardiography:

Echocardiographic studies were performed at baseline and after 7, 28, 56 days of coronary occlusion using the Vevo 2100 system (VisualSonics. Toronto ON), as previously described[15]. Long-axis B-mode was used to assess the geometric characteristics of the left ventricle after myocardial infarction. Short-axis M-mode was used for measurement of systolic and diastolic ventricular diameters and wall dimensions. The left ventricular end-diastolic diameter (LVEDD), left ventricular end-systolic diameter (LVESD), left ventricular end-systolic volume (LVESV), and left ventricular end-diastolic volume (LVEDV) were measured as indicators of dilative remodeling. Left ventricular mass (LV mass) was measured as an indicator of hypertrophic remodeling. The left ventricular ejection fraction (LVEF = [(LVEDV-LVESV) / LVEDV] × 100%) was measured for assessment of systolic ventricular function.

Immunohistochemistry and quantitative histology:

For histopathological analysis, mouse hearts were fixed in zinc-formalin (Z-fix; Anatech, Battle Creek, MI), and embedded in paraffin. Infarcted hearts harvested after 7 or 56 days of coronary occlusion were sectioned from base to apex at 250 μm intervals, thus reconstructing the whole heart, as previously described [15,40]. 20 sections (5μm thick) were cut at each level. To assess the size of the infarct, the first section at each partition was

stained with hematoxylin and eosin (H&E). Morphometric parameters were quantitatively assessed using Axiovision software. The infarcted and non-infarcted areas were measured at each level and the volume of the infarct and of the non-infarcted remodeling myocardium at each level was calculated as: Infarct volume= infarct area*350μm (250μm+20sections*5μm=350μm) and volume of non-infarcted myocardium=non-infarcted area*350μm. The total volume of the infarcted and non-infarcted myocardium was calculated as the sum of the volumes of each partition. Scar size was measured by dividing the volume of the infarct by the total volume of the left ventricle (infarct volume+volume of non-infarcted myocardium), and was expressed as a percentage. In order to quantitatively assess scar remodeling in the infarcted heart, we measured at each partition 3 infarct thickness parameters: a) the smaller thickness for each level (Tlmin), b) the largest thickness for each level (Tlmax) and c) the infarct thickness at the midpoint between the areas of lowest and largest thickness (Tlmid). For each infarcted mouse, the smallest of the Tlmin values from all levels is the minimal thickness of the infarct (Tmin), and the highest of the Tlmax values is the maximal thickness of the infarct (Tmax). In order to quantify the average thickness of the infarct, a mean thickness was measured at each level (Tlmean) as Tlmean=(Tlmin+Tlmax+Tlmid)/3. The mean thickness for each infarct was quantified as the mean of all the Tlmean values. Picrosirius red staining was used to label the collagen-based scar.

Machine learning-based quantitative analysis of collagen surface area:

In order to assess collagen deposition following myocardial infarction, an artificial intelligence (AI)-based model was trained to segment Sirius red stained fibers using Intellesis module of Zen Pro software (Carl Zeiss Microscopy, New York NY). Image Analysis module of Zen Pro software was then used to incorporate analysis parameters in the trained AI model to measure surface areas of the segmented collagen fibers of the remote and infarcted areas at 7 and 56 days following myocardial infarction. At least 10 different fields from three non-adjacent stained sections per mouse at 3 different levels (basal, mid-myocardial, and apical levels) were scanned and analyzed per heart sample.

Immunofluorescence staining:

In order to systematically characterize the time course of Smad7 expression in infarct macrophages, Smad7 (using an anti-Smad7 antibody by Thermo Fisher Scientific, #42-0400) and GFP staining (using an anti-GFP antibody, Abcam, #ab6662) was performed on the infarcted $CSF1R^{EGFP}$ heart at baseline, 24h, 3-day, 7-day and 28-day timepoints (n=5-6/each time point). In order to identify myofibroblasts in the infarct, sections were stained with an anti-α-smooth muscle actin (SMA) antibody (Sigma, #F3777) as previously described[41]. Myofibroblasts were identified as spindle-shaped α-SMA-positive cells located outside the vascular media. To determine the number of macrophages in the infarcted and remodeling myocardium, sections from infarcted Smad7 fl/fl and MyS7KO mice were stained with an anti-Mac2 (galectin-3) antibody (Cedarlane, #CL8942AP), as previously described[42,43]. Quantitative analysis was performed by counting the number of macrophages in 10 fields from 2 different levels for each animal.

Machine learning-based quantitative analysis of myofibroblast density:

Using default algorithms of the Intellesis Trainable Segmentation module of Zen Pro software (Carl Zeiss Microscopy, New York NY), an AI-based model was trained on multiple fields of different regions of the myocardium to identify myofibroblasts. Objects of interest were defined as the DAPI-positive nuclei surrounded by α-SMA profiles, excluding vascular smooth muscle cells (VSMCs). The unstained myocardium and VSMCs were considered the background. Image Analysis module was then used to incorporate analysis settings in the trained model to count the segmented objects. Quantitative analysis was performed by counting the number of myofibroblasts in 10 fields from 2 different levels for each animal using the trained models.

Isolation, culture and stimulation of mouse BMMs:

Tibial bone marrow-derived macrophages were isolated from 2 month-old global inducible Smad7 KO mice, or corresponding Smad7 fl/fl animals, as previously described[15]. Briefly, bone marrow cells were incubated for 24 h in α+ MEM medium (GIBCO) supplemented with 15% fetal calf serum (GIBCO), and 12 ng/ml CSF-1 (R&D systems). Non-adherent primitive mononuclear phagocytes were reseeded in media containing 15% fetal calf serum and CSF-1 (120 ng/ml) for 48 hours, in order to allow their differentiation to adherent macrophages. Cells were cultured until confluent, starved in media without serum for approximately 16 hours, and then stimulated with TGF-β1 (10 ng/ml), TGF-β2 (10 ng/ml), TGF-β3 (10 ng/ml), BMP2 (50 ng/ml), BMP4 (50 ng/ml), BMP6 (50 ng/ml) or BMP7 (50 ng/ml) (all human cytokines from R&D systems) for 4h or 24h to examine Smad7 expression by BMMs. In order to determine the effect of Smad7 loss on inflammatory gene transcription in the presence of pro-inflammatory cytokines, control (Smad7 fl/fl) and Smad7 KO bone marrow macrophages were pre-treated with TGF-β1 (10ng/ml) for 2 hours, followed by stimulation with TNF-α (10ng/ml) for 4 hours. RNA was isolated using TRIzol reagent (Qiagen, #79306) and the RNA obtained was used for q-PCR or RNAseq.

RNA extraction, qPCR and PCR array:

Total RNA was extracted from cells, cDNA was amplified using the SsoFast EvaGreen Supermix reagent and the C1000 thermal cycler apparatus from Bio-Rad following the manufacturer's recommendations. The following primer pairs were used for qPCR: *Gapdh* forward 5'-AGGTCGGTGTGAACGGATTTG-3', *Gapdh* reverse 5'-TGTAGACCATGTAGTTGAGGTCA-3', *ActB* forward 5'-AACAGTCCGCCTAGAAGCAC-3', *ActB* reverse 5'-CGTTGACATCCGTAAAGACC-3', *Smad7* forward 5'-CTGCAACCCCCATCACCTTA-3', *Smad7* reverse 5'-CAGCCTGCAGTTGGTTTGAG-3', *Pdgfa* forward 5'- GGAACACCTGGAGTGTGCAT-3', and *Pdgfa* reverse 5'-CGGCTCATCTCACCTCACAT-3'. The housekeeping genes *Gapdh* and *ActB* were used as internal controls. The qPCR procedure was repeated three times in independent runs; gene expression levels were calculated using the ΔCT method.

For PCR array, total RNA was extracted using the RNeasy mini kits (Qiagen, 74104). A total of 0.5 μg of RNA was transcribed into cDNA using the RT^2 first strand kit (Qiagen, 330404). Quantitative PCR was then performed using the RT^2 Profiler mouse Cytokines

& Chemokines (PAMM-150Z), or mouse Extracellular Matrix & Adhesion Molecules (PAMM-013Z) from Qiagen according to the manufacturer's protocol. The same thermal profile conditions were used for all primers sets: 95°C for 10 minutes, 40 cycles at 95°C for 15 seconds and 60°C for 1 minute. The data obtained were exported to the SABiosciences PCR array web-based template where it was analyzed using the ΔΔCt method.

Isolation of infarct macrophages from Smad7 fl/fl and MyS7KO mice:

Macrophage and neutrophil cell suspensions were obtained from infarcted S7fl/fl and MyS7KO hearts after 3 and 7 days of coronary occlusion. Briefly, infarcted heart tissue was minced and placed into a cocktail of 0.25 mg/ml Liberase Blendzyme 3 (Roche Applied Science), 20 U/ml DNase I (Sigma-Aldrich), 10 mmol/l HEPES (Invitrogen), and 0.1% sodium azide in HBSS with $Ca2^{+}$ and $Mg2^{+}$ (Invitrogen), and shaken at 37°C for 20 minutes for 3 times. Cells were then passed through a 40-μm nylon mesh and centrifuged (10 minutes, 500 g, 4°C). Up to 10^{8} cells were reconstituted with 200 μl MACS buffer (Miltenyi Biotec, 130-091-376) and incubated with 50 μl of anti-Ly6G biotin beads (Miltenyi Biotec, 130-092-332) at 4°C for 10min, and then incubated with 100 μl of anti-biotin microbeads for 15min. washed once and centrifuged. Resuspended cells went through a MACS Column (Miltenyi Biotec, 130-042-201) set in a MACS Seperator (Miltenyi Biotec, 130-090-312). The magnetically labeled Ly6G+ cells were retained on the column. Approximately 1 ml of MACS buffer was applied onto the column. Ly6G+ cells were flushed out by firmly pushing the plunger and collected for RNA extraction. Unlabeled cells that passed through were collected and washed once with PBS as the Ly6G− cells. Subsequently, Ly6G− cells were incubated with CD11b microbeads (Miltenyi Biotec cat. 130-049-601) at 4°C for 15 minutes (10ul of microbeads per 10^{7} Ly6G− cells in 90ul MACS buffer), and then washed once and centrifuged. Resuspended cells went through a MACS Column set in a MACS separator. The magnetically labeled $CD11b^{+}$ cells were retained on the column. Ly6G−/CD11b+ cells (macrophages) were flushed out and harvested for RNA isolation. Gene expression in macrophages harvested from Smad7 fl/fl and MyS7KO mice was compared after 3 and 7 days of coronary occlusion. In order to confirm deletion of SMAD7 protein in infarct macrophages, CD11b+/Ly6G− macrophages were isolated as described above from Smad7 fl/fl and MyS7KO mice 5-days after infarction and were used for protein extraction. SMAD7 expression levels were assessed using Western blotting.

Protein extraction and Western blotting:

Protein from cardiac macrophages and bone marrow macrophages was extracted in RIPA lysis buffer, including 0.5M EDTA, 1X Protease and Phosphatase Inhibitors. Equal amount of protein from each experimental group was fractionated by 10% Mini-PROTEAN® TGX™ Gel (Bio-Rad Laboratories, 456-1036) and transferred onto a PVDF membrane (Bio-Rad Laboratories, #1620177). Membranes were incubated overnight with primary antibodies at 4°C followed by the application of appropriate horse radish peroxidase (HRP)-conjugated secondary antibodies for 2 hours. Proteins were detected using Pierce™ ECL Western blot detection reagents (Thermofisher, #32106) and imaged by the ChemiDoc™ MP System (Bio-Rad Laboratories). Bands were densitometrically quantified by ImageJ and normalized to appropriate loading controls. The following antibodies were used: anti-SMAD7 (1:500, #sc-101152, Santa Cruz) and anti-GAPDH (1:4000, #PA1-987, Invitrogen).

Flow cytometric sorting of infarct macrophages:

In order to examine the time course of Smad7 expression in infarct macrophages, cardiac CD11b+/Ly6G− macrophages were harvested through flow cytometric sorting from sham-operated or infarcted hearts of male C57BL/6 mice. Briefly, heart tissue was minced and placed into a cocktail of 0.25 mg/ml Liberase Blendzyme 3 (Roche Applied Science), 20 U/ml DNase I (Sigma-Aldrich), 10 mmol/l HEPES and 0.1% sodium azide in HBSS with Ca^{2+} and Mg^{2+}, and shaken at 37°C for 15 minutes twice, then cells were passed through a 40-μm nylon mesh and collected for centrifugation (10 minutes, 300 g, 4°C), followed by red blood cell lysis. Up to 10^8 cells were resuspended with 200 μl staining buffer and incubated with 20 μl of FITC anti-mouse/human CD11b Antibody (Biolegend, clone 1A8, cat# 101206) and 40 μl of Pacific Blue™ anti-mouse Ly-6G Antibody (Biolegend, clone M1/70, cat# 127612) at 4°C for 30min, then washed, centrifuged and resuspended for FACS sorting (BD FACSAria™II). The sham-operated heart was individually digested to single cells, and sorted macrophages from 8-10 hearts were pooled together for each sham sample. After 3, 7 or 14 days following myocardial infarction, infarcted heart including infarct zone and border zone, but excluding remote area tissue, were harvested for digestion. Total RNA was extracted from FACS-sorted CD11b+/Ly6G− macrophages using TRIzol Reagent (Invitrogen). *Smad7* expression levels in infarct macrophages were assessed using qPCR.

Library preparation for transcriptome sequencing:

RNA from cardiac macrophages from control Smad7 fl/fl and MyS7KO hearts, and infarct macrophages harvested from MyS7KO and Smad7 fl/fl mice after 3 and 7 days of coronary occlusion was used for RNA-seq, in order to investigate the effects of Smad7 loss on the transcriptional profile of cardiac macrophages in homeostasis and disease. Moreover, in order to study the effects of *Smad7* loss on the transcriptional profile of macrophages, RNA was isolated from unstimulated Smad7 control macrophages (WT-C), TGF-β1 treated Smad7 control macrophages (WT-TGF-β), unstimulated Smad7 KO macrophages (S7KO-C) and TGF-β1 treated Smad7 KO macrophages (S7KO-TGF-β). The samples were sent to Novogene (Sacramento, California) to construct cDNA libraries by using NEBNext® Ultra™ RNA Library Prep Kit for Illumina® (NEB, Ipswich, MA, USA).

In brief, the process of library construction consisted of i) mRNA purification and enrichment from total RNA using oligo(dt)-attached magnetic beads, ii) fragmentation of purified mRNA using divalent cations exposed to elevated temperatures in NEBNext First Strand Synthesis Reaction Buffer, iii) double stranded cDNA synthesis, using RNase H- reverse transcriptase (first strand) and DNA polymerase I, dNTP and RNase H (second strand); iv) terminal cDNA ends reparation by exonucleases/polymerases; and poly adenylation of the 3’ ends of the DNA fragments, v) sequencing adaptors ligation, and vi) cDNA fragments size selection (150-200 bp in length) which underwent PCR. PCR was performed using Phusion High-Fidelity DNA Polymerase, universal PCR primers and Index (X) Primer. PCR products were purified (AMPure XP system), and the library concentration (>2 nM) and quality were assessed using a Bioanalyzer 2100 system (Agilent, Santa Clara, CA, USA).

Quality analysis, mapping and assembly:

The library preparations were sequenced on Illumina Novaseq 6000 devices, generating 150 bp paired-end reads. Adapter, poly-N and low-quality reads from the raw data were excluded to purify the data analysis. Quality Phred Scores, Q20%, Q30% and GC contents of the clean data were calculated, showing high accuracy of reads (>99%, with 0.02 error rate). Filtered reads were aligned to the C57BL/6J reference genome (December 2011 release of the mouse musculus reference genome (mm10; GRCm38.p6) from Ensembl) using TopHat2 algorithm alignment program v.2.0.9 [44]. Mapped reads were assembled using both Scripture (beta2) and Cufflinks v.2.1.1 algorithm[45].

Gene expression, differential expression, enrichment and co-expression analysis:

HTSeq software v.0.6.1[46] was used to count the number of reads mapped to each gene. Read count of fragments per kilobase of transcript sequence per millions base pairs sequenced (FPKM), was used to calculate gene expression level, which considered the effects of both sequencing depth and gene length [45]. Readcount obtained from the gene expression analysis was used for differential expression analysis. Cluster differential expression analysis for every gene in the four different cardiac fibroblast conditions was performed using the DESeq2 R software package (v.1.10.1)[47]. Genes with an adjusted P-value ≤ 0.05 were considered to be differentially expressed. List of genes were ranked by differential gene expression as log2 (fold change) between each comparison group. Positive values were upregulated genes, whereas negative values were downregulated genes.

Top biological functions and canonical pathways associated with the differentially expressed mRNAs data set were identified with Ingenuity Pathway Analysis (IPA) (Qiagen). By comparing the imported RNA-seq data generated in the Agilent platform with Ingenuity® Knowledge Base, a list of relevant networks, upstream regulators and algorithmically generated mechanistic networks based on their connectivity was obtained. A score (p-score = − log10 (p-value)) according to the fit of the set of supplied genes and a list of biological functions stored in the Ingenuity Knowledge Base were generated. Only genes with a fold change of 1.0 and p-value ≤ 0.05 were considered. All RNA-seq processed data have been deposited in NCBI's Gene Expression Omnibus (GEO) and are accessible through GEO SuperSeries accession number GSE189451 (https://www.ncbi.nlm.nih.gov/geo/query/acc.cgi?acc=GSE189451).

Statistical analysis:

For all analyses, normal distribution was tested using the Shapiro-Wilk normality test. For comparisons of two groups, unpaired two-tailed Student's t test using (when appropriate) Welch's correction for unequal variances was performed. The Mann-Whitney test was used for comparisons between two groups that did not show Gaussian distribution. For comparisons of multiple groups, one-way ANOVA was performed followed by Sidak's or Tukey's multiple comparison post-hoc tests. The Kruskal-Wallis test, followed by Dunn's multiple comparison posttest was used when one or more groups did not show Gaussian distribution. Survival analysis was performed using the Kaplan-Meier method. Mortality was compared using the log rank test. Data were expressed as means ± SEM. Statistical significance was set at $P < 0.05$.

RESULTS

1. All 3 TGF-β isoforms induce Smad7 synthesis in isolated BMMs.

The I-Smads are induced by members of the TGF-β superfamily and have been suggested to serve as a negative feedback mechanism that restrains TGF-β-mediated signaling[31]. Accordingly, we examined the effects of TGF-β superfamily members on *Smad7* expression levels in mouse BMMs. All 3 TGF-β isoforms (TGF-β1, TGF-β2 and TGF-β3) induced Smad7 upregulation (Figure 1A) after 4h of stimulation. In contrast, BMP2, BMP4, BMP6 and BMP7 had no significant effects on *Smad7* mRNA expression (Figure 1A). In order to examine whether longer stimulation with BMPs induces *Smad7* expression, we stimulated BMMs for 4 and 24h with TGF-β1, BMP2 and BMP4. TGF-β1 markedly upregulated *Smad7* at both 4 and 24h timepoints; in contrast, the BMPs had no effect on *Smad7* transcription (Figure 1B). In contrast, expression of *Pdgfa*, a gene known to be upregulated by TGF-β superfamily members in several different cell types [48],[49] was induced in BMMs by both TGF-β1 and BMP4 after 4h of stimulation (Figure 1C).

2. Smad7 expression in tissue macrophages

Macrophages are heterogeneous, exhibiting tissue-specific transcriptomic and functional profiles. In order to examine *Smad7* expression patterns in mouse macrophages from different organs, we analyzed data from the ImmGen ULI database: OpenSource Mononuclear Phagocytes Project (GSE122108)[50]. Microglial macrophages exhibited the highest levels of *Smad7* expression, followed by $CCR2^{+}$ and $CCR2^{-}$ cardiac macrophages. In contrast, aortic, peritoneal, renal, spleen macrophages and circulating blood monocytes had low baseline levels of *Smad7* expression (Figure 1D).

3. Smad7 is upregulated in macrophages infiltrating the infarcted myocardium after 7 days of coronary occlusion.

Because TGF-β isoforms upregulate macrophage Smad7 synthesis (Fig 1), and myocardial infarction is associated with marked induction and activation of TGF-βs[15], we hypothesized that Smad7 may be upregulated in infarct macrophages. In order to localize Smad7 in infarct macrophages, we used $CSF1R^{EGFP}$ macrophage reporter mice (Figure 2). Low levels of Smad7 immunoreactivity were noted in control mouse hearts (Figure 2A–C). Following myocardial infarction, Smad7 immunoreactivity was markedly increased in the infarct zone, and was localized in interstitial cells and in border zone cardiomyocytes (Figure 2D–L). $CSF1R^{+}$ macrophages infiltrated the infarcted heart after 24h, and peaked after 7 days of coronary occlusion (Figure 2P). The density of Smad7-expressing $CSF1R^{+}$ macrophages significantly increased after 3 days, and peaked after 7 days of coronary occlusion (Figure 2Q). Although the percentage of Smad7-expressing macrophages remained high at the 28-day timepoint, the density of Smad7-expressing macrophages decreased, reflecting a reduction in macrophage infiltration (Figure 2M–R).

Cellular Smad7 levels are regulated through transcription and via post-transcriptional mechanisms that modulate protein degradation[51]. In order to examine whether infarct macrophages have increased Smad7 transcription, we assessed *Smad7* levels in FACS-sorted CD11b+/Ly6G− macrophages harvested from sham hearts and from infarcted hearts after 3,

7 and 14 days of coronary occlusion (Figure 2S). ANOVA showed a significant change in the levels of Smad7 expression in infarct macrophages (ANOVA p value 0.048). *Smad7* expression was increased by ~50% in infarct macrophages at the 7-day timepoint, in comparison to 3-day infarct macrophages (p=0.0496, Tukey post-hoc test, n=4/group), and to macrophages harvested from sham hearts (p=0.0977, Tukey correction, n=3-4/group) (Figure 2T). Thus, the increased infiltration of the infarcted heart with SMAD7+ macrophages may involve, at least in part, transcriptional upregulation of *Smad7*.

4. Myeloid cell-specific Smad7 loss has no significant effects on homeostasis.

In order to study the role of Smad7 in regulating macrophage phenotype following myocardial infarction, we generated myeloid cell-specific Smad7 KO mice using the lysozyme-M Cre driver. We documented loss of Smad7 in infarct macrophages harvested from MyS7KO mice both at the RNA and protein level. First, CD11b+/Ly6G− macrophages, CD11b−/Ly6G+ neutrophils and CD11b−/Ly6G− non-myeloid interstitial cells were harvested from the infarcted heart of MyS7KO and Smad7 fl/fl mice, 3 days after permanent coronary occlusion. Macrophages (Fig 3A), but not neutrophils (Figure 3B) and non-myeloid interstitial cells (Figure 3C) harvested from MyS7KO infarcts exhibited a marked reduction in *Smad7* expression, when compared to cells harvested from Smad7 fl/fl infarcts (Figure 3). Next, we extracted protein from BMMs obtained from MyS7KO and Smad7 fl/fl mice. MyS7KO BMMs had a marked reduction in SMAD7 levels when compared with Smad7 fl/fl cells (Figure 3D–E). Finally, infarct macrophages were harvested from Smad7 fl/fl and MyS7KO animals undergoing 5-day coronary occlusion protocols. MyS7KO infarct macrophages had a marked reduction in SMAD7 levels when compared with Smad7 fl/fl cells ($p<0.0001$ n=4–7/group, Figure 3F–H). The specificity of the SMAD7 antibody was confirmed using protein extracted from the spleen of mice with global inducible Smad7 deletion (Figure 3D, F–G).

Myeloid cell-specific Smad7 loss had no significant effects on homeostasis. Body weight was comparable between MyS7KO and Smad7 fl/fl mice (Supplemental Figure I). Moreover, MyS7KO mice and corresponding Smad7 fl/fl controls had comparable baseline echocardiographic parameters, suggesting no significant effects of macrophage-specific Smad7 loss on cardiac function, chamber dimensions and LV mass (Supplemental Figure II). We also examined the effects of *Smad7* loss on the transcriptome of cardiac macrophages using RNA-seq. Based on a $p<0.05$, 282 genes were differentially expressed in *Smad7* KO macrophages. 185 were downregulated in *Smad7* null cells in comparison to Smad7 fl/fl cells, whereas 97 genes were upregulated. None of the genes were >2-fold or <0.5fold, and had a padj<0.05 (Supplemental Figure III). Pathway enrichment analysis did not identify any pathways differentially regulated in *Smad7* KO cells, supporting the notion that endogenous *Smad7* expression does not affect the transcriptional profile of normal resident cardiac macrophages.

5. The effects of myeloid cell-specific Smad7 loss on the gene expression profile of infarct macrophages.

Next, we examined whether induction of Smad7 following infarction plays a role in macrophage phenotypic transitions, thus regulating the inflammatory, reparative and

remodeling responses following myocardial infarction. Smad7 loss was associated with a much higher number of differentially regulated genes in infarct macrophages than in control hearts, likely reflecting the importance of Smad7 in regulation of macrophage phenotype following injury. 3 days after myocardial infarction, Smad7 KO macrophages exhibited upregulation of 291 genes and downregulation of 464 genes, whereas at the 7-day timepoint 867 genes were upregulated and 613 genes were downmodulated (Fig 4A–D). IPA of the transcriptomic data at the 7-day timepoint identified 3 canonical pathways that were differentially regulated by Smad7 loss (absolute z score >2). The semaphorin pathway was predicted to be activated in Smad7 KO cells, whereas TREM1 signaling and oxidative phosphorylation were predicted to be inhibited (Figure 4E). Furthermore, analysis of diseases and cellular functions differentially regulated by Smad7 loss, predicted inhibition of myeloid cell chemotaxis in Smad7 KO macrophages (Supplemental Table 1) and activation of pathways involved in microtubule dynamics, cytoskeletal organization and formation of cellular protrusions (Supplemental Table 2).

6. Myeloid cell-specific Smad7 loss does not affect mortality and adverse remodeling following myocardial infarction

Next, we asked whether the transcriptomic changes noted in Smad7 KO infarct macrophages are associated with effects in cardiac dysfunction, repair, remodeling and fibrosis of the infarcted heart. During the first week after coronary occlusion, C57Bl6 mice exhibit significant mortality which is predominantly noted in male animals. ~50% of the deaths during the first week post-infarction are caused by left ventricular rupture[52]. Myeloid cell-specific Smad7 loss did not affect mortality rates in both male and female mice (Figure 5A–C). In order to examine the effects of myeloid cell-specific Smad7 loss on post-infarction dysfunction and adverse remodeling, we performed echocardiographic studies at 7, 28 and 56-day timepoints after coronary occlusion. MyS7KO and Smad7 fl/fl mice had comparable ejection fraction after 7, 28 and 56 days of coronary occlusion, suggesting that myeloid cell-specific Smad7 loss has no significant effects on systolic dysfunction after myocardial infarction (Figure 5D). Moreover, *Smad7* loss did not significantly affect LVEDD, LVEDV, and LVESD after 7-56 days of coronary occlusion (Figure 5E–G). LVESV was modestly, but significantly lower in MyS7KO mice at the 28-day timepoint; however, no significant effects of myeloid cell-specific Smad7 loss on LVESV were noted at the 7 and 56-day timepoints (Figure 5H). Left ventricular anterior wall thickness was comparable between groups at all timepoints (Figure 5I). Overall, systematic echocardiographic analysis showed no significant effects of myeloid cell-specific Smad7 loss on dysfunction and adverse remodeling of the infarcted heart.

7. Myeloid cell-specific Smad7 loss does not significantly affect scar size and scar remodeling following myocardial infarction

In order to examine the effects of myeloid cell-specific Smad7 loss on scar size and remodeling following infarction, we performed systematic analysis of morphometric parameters, by sectioning the entire ventricle from base to apex (Figure 6A). As the scar matures, thinning of the infarcted segments is noted, leading to marked reduction in scar size and decreased mean and minimal infarct thickness 56 days after myocardial infarction (Figure 6B–D). Myeloid cell-specific Smad7 loss had no effects on scar size and on the

minimal thickness of the scar at the 7- and 56-day timepoints (Figure 6B–C). At the 7-day timepoint, mean infarct thickness was modestly, but significantly higher in MyS7KO mice; however, 56 days after coronary occlusion, no significant difference was noted between MyS7KO and Smad7 fl/fl scars (Figure 6D).

8: Myeloid cell-specific Smad7 loss does not affect macrophage density in the healing infarct and in the remote remodeling myocardium.

Next, we examined whether myeloid cell-specific Smad7 loss affects macrophage infiltration in the infarcted myocardium. Macrophages in the infarcted and remodeling heart were identified using Mac2 immunofluorescence. MyS7KO mice and corresponding Smad7 fl/fl controls had comparable macrophage density in the infarct zone and in the remote remodeling myocardium 7-56 days after coronary occlusion (Supplemental figure IV)

9. Myeloid cell-specific Smad7 loss does not affect collagen deposition in the infarcted myocardium, but is associated with a transient reduction in myofibroblast density 7 days after myocardial infarction

Macrophages are involved in regulation of the fibrotic response by secreting mediators that modulate fibroblast function and by contributing to matrix remodeling through secretion of proteases and anti-proteases. In order to examine whether Smad7 plays a role in regulation of the fibrogenic properties of infarct macrophages, we assessed the effects of myeloid cell-specific Smad7 loss on myofibroblast infiltration and on collagen deposition in the infarcted heart. Myofibroblasts were identified in the infarcted myocardium as α-SMA-immunoreactive cells located outside the media of vessels (Figure 7A). Myofibroblast density was modestly but significantly lower in MyS7KO infarcts, in comparison to Smad7 fl/fl infarcts (Figure 7C) at the 7-day timepoint. However, the effect of Smad7 loss on myofibroblast density was transient; at the 56-day timepoint, myofibroblast density was comparable between groups. Picrosirius red staining was used to assess collagen content in the infarcted and remodeling myocardium (Figure 7B, D). Quantitative analysis showed no significant effects of myeloid cell-specific Smad7 loss on collagen deposition in the infarct zone and in the remodeling myocardium at both timepoints examined (Figure 7D).

In order to examine whether the absence of significant effects of myeloid cell-specific Smad7 loss on post-infarction remodeling and dysfunction may be due to compensatory actions of the other inhibitory Smad, Smad6, we compared *Smad6* levels in Smad7 fl/fl and MyS7KO infarct macrophages using RNA-seq. Smad7 loss did not affect *Smad6* expression levels in infarct macrophages (Supplemental Figure V). Moreover, no significant effects of Smad7 loss were noted on expression of genes involved in TGF-β superfamily signaling, such as the genes encoding TGF-β receptors, the Receptor-activated Smads and Smurf1/2 (Supplemental Table 3).

Thus, in summary, our in vivo experiments showed no significant effects of macrophage-specific Smad7 loss on post-infarction inflammation and adverse remodeling. A modest, but significant effect of Smad7 loss on early myofibroblast infiltration was not associated with any consequences on ventricular function.

10. Smad7 does not affect the anti-inflammatory effects of TGF-β in BMMs.

Because Smad7 has been suggested to modulate macrophage inflammatory activity, we examined the in vitro effects of Smad7 on inflammatory gene synthesis by isolated BMMs. Smad7 KO BMMs were harvested from young mice with global inducible loss of Smad7. These animals exhibited no baseline defects. Smad7 KO and control macrophages were stimulated with TGF-β1 (10ng/ml) for 4h. Loss of *Smad7* in Smad7 KO bone marrow macrophages was confirmed, using qPCR (Figure 8A). Expression levels of inflammatory mediators was assessed using a PCR array (Figure 8, Supplemental Figure VI, Supplemental Table 4). Smad7 KO cells had higher baseline expression of *Tnfa* (Figure 8B) and *Tnfsf10* (Figure 8D), and lower baseline expression of *Ccl2* (Figure 8E). Smad7 loss did not affect the anti-inflammatory actions of TGF-β on expression of inflammatory cytokines (*Tnfa, Tnfsf4, Tnfsf10*, Figure 8B–D) and chemokines (*Ccl2, Ccl3, Ccl4*, Figure 8E–G). Moreover, Smad7 loss had no significant effects on the potent suppressive actions of TGF-β1 on synthesis of IL-6 signal transducer (*Il6st*, Figure 8H).

Next, we examined whether Smad7 modulates inflammatory gene synthesis in the presence of pro-inflammatory cytokines. TNF-α-stimulated WT and Smad7 KO BMMs were pre-treated with TGF-β1, and gene expression was assessed using a PCR array (Figure 9, Supplemental Figure VII, Supplemental Table 5). TGF-β1 markedly suppressed inflammatory chemokine (*Ccl2, Ccl3, Ccl4, Ccl5, Ccl6, Ccl9, Ccl12, Pf4, Cxcl10*) and cytokine (*Bmp2, Tnfa, Tnfsf10*) gene expression (Figure 9A–L) in both WT and Smad7 KO cells, suggesting that Smad7 does not play a role in regulation of the anti-inflammatory actions of TGF-β in macrophages. In contrast to its suppressive effects on expression of a wide range of pro-inflammatory cytokines, TGF-β1 upregulated synthesis of *Tnfsf13b*, *Osm* and *Vegfa* (Fig 9M–O). However, Smad7 loss did not affect expression of these genes in BMMs. Thus, Smad7 does not inhibit the de-activating anti-inflammatory actions of TGF-β on cytokine-stimulated macrophages.

11. Effects of Smad7 on expression of matrix remodeling genes in BMMs.

Macrophages are involved in matrix remodeling by secreting matrix-degrading proteases, anti-proteases and matricellular proteins. In order to examine the role of Smad7 in regulating the fibrogenic properties of macrophages, we performed a PCR array focusing on levels of fibrosis and extracellular matrix-related genes (Figure 10, Supplemental Figure VIII, Supplemental Table 6). TGF-β stimulation induced expression of the integrins *Itga5*, *Itgal* and *Itgav* (Figure 10A–C), had no significant effects on *Itgb1* levels (Figure 10D) and downregulated *Itgb3* synthesis (Figure 10E). Smad7 loss was associated with modest, but significant accentuation of TGF-β-induced *Itga5* expression, without significantly affecting the effects of TGF-β on other integrins.

TGF-β also suppressed *Mmp13* expression (Figure 10F), markedly induced *Mmp2* (Figure 10H) and downregulated *Mmp9* expression (Figure 10I) in both WT and Smad7 KO macrophages. Smad7 loss was associated with significantly increased baseline expression levels of *Mmp14* (Figure 10G); however, *Mmp* levels were comparable between TGF-β-stimulated WT and Smad7 KO cells. TGF-β also markedly induced expression of the matricellular protein *Tgfbi* (Figure 10J) and suppressed levels of the adhesion molecules

Icam1 (Figure 10K) and *Vcam1* (Figure 10L) in both WT and Smad7 KO cells. Smad7 loss did not affect expression levels of *Tgfbi*, *Vcam1* and *Icam1* in BMMs. Thus, our findings suggest that Smad7 has no significant effects in regulation of the matrix-remodeling properties of TGF-β-stimulated macrophages.

12. Effects of Smad7 loss on the transcriptome of TGF-β-stimulated macrophages.

Our PCR array data showed that macrophage Smad7 has very limited impact on expression of genes associated with inflammation and ECM remodeling. In order to explore effects of Smad7 on other TGF-β inducible genes in macrophages, we performed RNA-seq. TGF-β stimulation markedly altered the transcriptome of BMMs, inducing 1338 genes and downmodulating 1267 genes (Figure 11A). IPA analysis suggested that TGF-β stimulation regulates numerous pathways (Supplemental Figure IX). The top pathways (z-score>2) activated by TGF-β stimulation in macrophages included sphingosine 1-phosphate, integrin signaling, Gβγ signaling, Wnt-β-catenin signaling, and LXR/RXR activation. The top pathways predicted to be inhibited by TGF-β (z-score<−2) included cholesterol biosynthesis pathways, G1/S checkpoint regulation, retinoid acid mediated apoptosis, BAG2 signaling, LPS/IL1-mediated RXR function, and the superpathway of geranylgeranyl-diphosphate signaling (Supplemental Figure IX). Smad7 absence had modest effects on the macrophage transcriptome in both unstimulated and TGF-β-stimulated cells (Fig 11B–C). In unstimulated cells, Smad7 absence was associated with upregulation of 18 genes and downregulation of 31 genes (Figure 11B). In TGF-β-stimulated cells, Smad7 loss was associated with induction of 10 genes and downmodulation of 18 genes (Figure 11C). Gene-specific analysis (Figure 12) showed that Smad7 loss suppressed baseline expression of *Pomk* and *Tepcr1* (Figure 12C–D). *Smad7* restrained expression of the TGF-β-induced genes *Fabp7* and *Olfml3* (Figure 12E–F), and mediated synthesis of the TGF-β-induced genes *Fn1, Ccdc107, Prickle2, Nav2*, and *C77080)* (Figure 12G–K). Moreover, Smad7 was found to stimulate expression of several genes, which are not induced by TGF-β (*Adam19, Bsn, Colec12*, and *Rps3a1*) (Figure 12L–O). However, none of these genes was modulated by Smad7 loss in infarct macrophages (padj>0.05).

DISCUSSION:

We report the first systematic study on the role of Smad7 in regulation of macrophage phenotype in homeostasis and disease. We show that in normal mice, *Smad7* is expressed in macrophages in a tissue-specific manner. Following myocardial infarction, macrophages exhibit a marked increase in SMAD7 expression, that peaks during the proliferative phase of infarct healing (Figure 2). Although myeloid cell-specific Smad7 loss has significant effects on the transcriptomic profile of infarct macrophages, these alterations only have modest and transient effects on the cellular composition of the infarct, and are not associated with effects on cardiac function and adverse post-infarction remodeling (Figure 4–5). In vitro, TGF-β exerts potent anti-inflammatory effects on cytokine-stimulated macrophages, stimulates integrin synthesis and modulates expression of matrix-remodeling genes. However, endogenous Smad7 has very limited effects on the transcriptional profile of bone marrow macrophages, in the presence or absence of TGF-β. Our study addresses the controversy on the role of endogenous Smad7 in inflammatory and immune

responses, which is driven by conflicting data suggesting both pro-inflammatory[34] and anti-inflammatory[35,36] effects. Our in vivo data suggest that the effects of Smad7 on macrophage gene expression have limited impact on tissue repair. Moreover, our in vitro experiments show minimal effects of Smad7 in regulation of TGF-β responses in macrophages.

TGF-β signaling cascades regulate macrophage phenotype in the infarcted and remodeling heart

The adult myocardium contains a population of resident macrophages[3,4] that expands following myocardial infarction through recruitment of circulating monocytes[6,3,4]. Infarct macrophages exhibit remarkable heterogeneity and undergo dramatic phenotypic changes during the phases of cardiac repair, in response to alterations in their microenvironment[53, 54,55]. Initiation of the inflammatory phase after myocardial infarction is triggered by tissue resident CCR2+ macrophages, which activate MyD88 signaling, and serve as an important source of pro-inflammatory cytokines and chemokines, orchestrating new recruitment of leukocytes[56,9]. In the infarct, infiltrating macrophages phagocytose dead cells and matrix debris, thus setting the stage for replacement of dead myocardium with a collagen-based scar[14]. As macrophages ingest apoptotic cells, they undergo anti-inflammatory transition, secreting IL-10[57], TGF-β[6] and matricellular proteins (such as osteopontin[58,59]), and promoting myofibroblast activation[16,60]. In addition to their fibroblast-activating functions, infarct macrophages also stimulate angiogenesis by secreting angiogenic mediators, such as VEGF[18] and endoplasmic reticulum membrane protein complex subunit 10 (EMC10)[61]. The phenotypic transitions of macrophages during the phases of infarct healing involve sequential recruitment of monocyte subsets with distinct properties[12], and temporally distinct patterns of stimulation with cytokines, growth factors and matricellular proteins.

TGF-β serves as a central regulator of monocyte and macrophage phenotype and function in many different pathologic conditions[21]. A large body of evidence suggests that the effects of TGF-β on mononuclear phagocytes are dependent on the state of differentiation of the cells. In monocytes, TGF-β exerts pro-inflammatory effects, acting as a monocyte chemoattractant[62], and upregulating expression of adhesion molecules[25]. In contrast, in mature macrophages, TGF-β exerts potent immunosuppressive[63], and anti-inflammatory effects, that have been attributed, at least in part, to inhibition of NF-κB signaling, through degradation of the adaptor protein MyD88[64]. Moreover, in vitro investigations have suggested a wide range of additional TGF-β effects on macrophages, including actions in recognition of apoptotic cells[65], pro-atherogenic stimulation[66], induction of CSF-1[67] (an effect that may promote their differentiation and proliferation[68]), stimulation of arginase activity[69], and modulation of MMP synthesis and activity[70]. Our studies have suggested that the effects of TGF-β on macrophages may predominantly involve Smad-dependent signaling cascades, and not Smad-independent pathways[15]. We demonstrated that activation of the Smad3 cascade in infarct macrophages promotes phagocytosis of dead cells, and is also implicated in anti-inflammatory transition, mediating synthesis of TGF-β and IL-10[15], and suppressing expression of pro-inflammatory mediators, such as IL-1β, TNF-α and CCL2[15]. Other investigations have suggested that, in addition to its anti-inflammatory effects, macrophage TGF-β/Smad3 signaling may also suppress synthesis of the metalloproteinase

MMP-12[71,72], while stimulating expression of the serine protease urokinase plasminogen activator (uPA)[73], and inducing release of angiogenic growth factors, such as VEGF[74].

The role of Smad7 in modulating the anti-inflammatory effects of TGF-β on macrophages

The inhibitory Smad, Smad7, serves as a potent endogenous negative regulator of TGF-β actions, restraining TGF-β signaling cascades in many different cell types[75,31,76,77]. In macrophages, the role of Smad7 as a negative regulator of TGF-β-mediated actions remains controversial, as various studies have produced conflicting results. Experiments in a viral infection model suggested that induction of Smad7 in macrophages may trigger inflammation, abrogating the anti-inflammatory effects of TGF-β[78]. In contrast, other investigations have suggested that Smad7 may inhibit inflammation. In a model of peritoneal inflammation, Smad7 overexpression attenuated inflammatory activity, reducing macrophage infiltration[79]. In a model of renal injury, Smad7 delivery was found to inhibit inflammation reducing accumulation of macrophages, through effects attributed to upregulation of IκBa and reduced NF-κB activation[34]. In a model of corneal injury, adenoviral transfer of Smad7 suppressed monocyte and macrophage influx, reducing synthesis of monocyte chemoattractant chemokines[80]. Whether these in vivo effects reflect direct anti-inflammatory actions of Smad7 on macrophages, or secondary effects due to modulation of the inflammatory profile of other cell types is unclear. Hong et al. demonstrated that in BMMs Smad7 mediates the anti-inflammatory actions of TGF-β, by binding to TAB2 and TAB3, two adaptor proteins that link the kinase TAK-1 with the pro-inflammatory TNF-α signaling cascade[33]. Formation of Smad7:TAB2 and Smad7:TAB3 complexes was suggested to inhibit TAK1 recruitment to TRAF2, thus blocking TNF/NF-κB signaling.

In contrast to these published findings, our experiments show that endogenous Smad7 has no significant effects in modulation of the anti-inflammatory actions of TGF-β in macrophages (Figure 9). Systematic assessment of inflammatory gene transcription using a PCR array and whole-transcriptome analysis with RNA-seq showed that Smad7 loss in macrophages had no significant effects on expression of inflammatory genes. The basis for the conflicting observations between our study and previously published observations on the effects of Smad7 in bone marrow macrophages is unclear, but may reflect different strategies for Smad7 knockdown, or the use of different endpoints for assessment of inflammatory activity. We used a highly-specific genetic approach to delete Smad7 in macrophages, and we systematically characterized the effects of Smad7 loss on the transcriptomic profile using PCR arrays and RNA-seq. In contrast, Hong et al used an siRNA knockdown approach that may have off-target effects, and assessed expression of a single inflammatory mediator, IL-6 [33].

Although Smad7 absence did not affect the anti-inflammatory actions of TGF-β, a small fraction of TGF-β-induced macrophage genes were restrained by Smad7 in vitro. *Olfml3* was induced upon TGF-β stimulation and was suppressed by Smad7 (Figure 12F). *Olfml3* encodes the protein olfactomedin like-3, which has been implicated in regulation of angiogenesis and pericyte proliferation[81,82]. Moreover, our PCR array data showed that expression of *Itga5* was modestly but significantly increased upon Smad7 loss in TGF-β-

stimulated macrophages (Figure 10A). Upregulation of integrin α5 in Smad7 null cells may accentuate responses of macrophages to integrin-binding extracellular matrix proteins, such as fibronectin. However, no significant effects of Smad7 loss on Olfml3 and Itga5 expression levels were noted in infarct macrophages.

The in vivo actions of macrophage Smad7 in healing myocardial infarction

Despite the absence of significant effects of endogenous Smad7 in vitro, myeloid cell-specific Smad7 loss had a significant impact on the transcriptional profile of infarct macrophages. RNA-seq analysis showed that Smad7 KO macrophages harvested 7 days after infarction exhibited upregulation of 867 genes and downregulation of 613 genes, in comparison to WT infarct macrophages isolated at the same timepoint. Bioinformatic analysis predicted inhibition of myeloid cell chemotaxis, associated with attenuated TREM1 signaling and activated semaphorin pathways in cells lacking Smad7. TREM1 has been previously reported to extend inflammatory injury in experimental models of myocardial infarction[83,84], stimulating chemokine synthesis and accentuating leukocyte recruitment in the infarcted myocardium. On the other hand, semaphorin 3a was found to exert anti-inflammatory actions, attenuating dysfunction after myocardial infarction[85]. However, despite the significant impact of Smad7 loss on the transcriptional profile of infarct macrophages, effects on the cellular inflammatory response were modest, and no effects on cardiac remodeling and dysfunction were noted. The transient reduction in myofibroblast infiltration observed in myeloid cell-specific Smad7 KO mice (Figure 7) may reflect the attenuated inflammatory activity of macrophages suggested by the RNA-seq data, but was not sufficient to affect remodeling and dysfunction of the infarcted heart.

Conclusions

We provide the first systematic in vivo and in vitro investigation on the role of endogenous macrophage Smad7 in homeostasis and ischemic injury. Although Smad7 is upregulated in macrophages after myocardial infarction, the role of macrophage-specific Smad7 in modulating the reparative response is limited. This finding contrasts the significant effects of myofibroblast Smad7 induction in restraining fibrosis, and in protecting from adverse remodeling after myocardial infarction[77]. The cell-specific effects of Smad7 in the infarcted myocardium may reflect differences in the levels of upregulation between cell types and the distinct roles of TGF-β-dependent and TGF-independent pathways modulated by Smad7 in fibroblasts and in macrophages.

Supplementary Material

Refer to Web version on PubMed Central for supplementary material.

ACKNOWLEDGMENTS:

Dr. Frangogiannis' laboratory is supported by NIH grants R01 HL76246, R01 HL85440, and R01 HL149407, and by Department of Defense grant PR181464. Dr. Humeres, Dr. Chen and Dr Hanna were supported by post-doctoral awards by the American Heart Association. Dr. Jun Li and Dr. Ruoshui Li were supported by the Chinese Scholarship Council. Dr Tuleta is supported by a post-doctoral grant from the Deutsche Forschungsgemeinschaft (TU 632/1-1).

DATA AVAILABILITY STATEMENT:

The data that support the findings of this study are available in the methods and/or supplementary material of this article. All RNA-seq processed data have been deposited in NCBI's Gene Expression Omnibus (GEO) and are accessible through GEO SuperSeries accession number GSE189451 (https://www.ncbi.nlm.nih.gov/geo/query/acc.cgi?acc=GSE189451)

REFERENCES:

1. Lavine KJ, Pinto AR, Epelman S, Kopecky BJ, Clemente-Casares X, Godwin J, Rosenthal N, Kovacic JC. The Macrophage in Cardiac Homeostasis and Disease: JACC Macrophage in CVD Series (Part 4). J Am Coll Cardiol. 2018; 72:2213–2230. [PubMed: 30360829]
2. Frodermann V, Nahrendorf M. Macrophages and Cardiovascular Health. Physiol Rev. 2018; 98:2523–2569. [PubMed: 30156496]
3. Epelman S, Lavine KJ, Beaudin AE, Sojka DK, Carrero JA, Calderon B, Brija T, Gautier EL, Ivanov S, Satpathy AT, et al. Embryonic and Adult-Derived Resident Cardiac Macrophages Are Maintained through Distinct Mechanisms at Steady State and during Inflammation. Immunity. 2014; 40:91–104. [PubMed: 24439267]
4. Heidt T, Courties G, Dutta P, Sager HB, Sebas M, Iwamoto Y, Sun Y, Da Silva N, Panizzi P, van der Laan AM, et al. Differential contribution of monocytes to heart macrophages in steady-state and after myocardial infarction. Circ Res. 2014; 115:284–295. [PubMed: 24786973]
5. Dick SA, Macklin JA, Nejat S, Momen A, Clemente-Casares X, Althagafi MG, Chen J, Kantores C, Hosseinzadeh S, Aronoff L, et al. Self-renewing resident cardiac macrophages limit adverse remodeling following myocardial infarction. Nat Immunol. 2019; 20:29–39. [PubMed: 30538339]
6. Dewald O, Zymek P, Winkelmann K, Koerting A, Ren G, Abou-Khamis T, Michael LH, Rollins BJ, Entman ML, Frangogiannis NG. CCL2/Monocyte Chemoattractant Protein-1 regulates inflammatory responses critical to healing myocardial infarcts. Circ Res. 2005; 96:881–889. [PubMed: 15774854]
7. Swirski FK, Nahrendorf M, Etzrodt M, Wildgruber M, Cortez-Retamozo V, Panizzi P, Figueiredo JL, Kohler RH, Chudnovskiy A, Waterman P, et al. Identification of splenic reservoir monocytes and their deployment to inflammatory sites. Science. 2009; 325:612–616. [PubMed: 19644120]
8. Frantz S, Hofmann U, Fraccarollo D, Schafer A, Kranepuhl S, Hagedorn I, Nieswandt B, Nahrendorf M, Wagner H, Bayer B, et al. Monocytes/macrophages prevent healing defects and left ventricular thrombus formation after myocardial infarction. FASEB J. 2013; 27:871–881. [PubMed: 23159933]
9. Huang CK, Dai D, Xie H, Zhu Z, Hu J, Su M, Liu M, Lu L, Shen W, Ning G, et al. Lgr4 Governs a Pro-Inflammatory Program in Macrophages to Antagonize Post-Infarction Cardiac Repair. Circ Res. 2020; 127:953–973. [PubMed: 32600176]
10. Sager HB, Hulsmans M, Lavine KJ, Moreira MB, Heidt T, Courties G, Sun Y, Iwamoto Y, Tricot B, Khan OF, et al. Proliferation and Recruitment Contribute to Myocardial Macrophage Expansion in Chronic Heart Failure. Circ Res. 2016; 119:853–864. [PubMed: 27444755]
11. DeBerge M, Glinton K, Subramanian M, Wilsbacher LD, Rothlin CV, Tabas I, Thorp EB. Macrophage AXL receptor tyrosine kinase inflames the heart after reperfused myocardial infarction. J Clin Invest. 2021; 131.
12. Nahrendorf M, Swirski FK, Aikawa E, Stangenberg L, Wurdinger T, Figueiredo JL, Libby P, Weissleder R, Pittet MJ. The healing myocardium sequentially mobilizes two monocyte subsets with divergent and complementary functions. J Exp Med. 2007; 204:3037–3047. [PubMed: 18025128]
13. Mia MM, Cibi DM, Abdul Ghani SAB, Song W, Tee N, Ghosh S, Mao J, Olson EN, Singh MK. YAP/TAZ deficiency reprograms macrophage phenotype and improves infarct healing and cardiac function after myocardial infarction. PLoS Biol. 2020; 18:e3000941. [PubMed: 33264286]

14. Wan E, Yeap XY, Dehn S, Terry R, Novak M, Zhang S, Iwata S, Han X, Homma S, Drosatos K, et al. Enhanced efferocytosis of apoptotic cardiomyocytes through myeloid-epithelial-reproductive tyrosine kinase links acute inflammation resolution to cardiac repair after infarction. Circ Res. 2013; 113:1004–1012. [PubMed: 23836795]
15. Chen B, Huang S, Su Y, Wu YJ, Hanna A, Brickshawana A, Graff J, Frangogiannis NG. Macrophage Smad3 Protects the Infarcted Heart, Stimulating Phagocytosis and Regulating Inflammation. Circ Res. 2019; 125:55–70. [PubMed: 31092129]
16. Petz A, Grandoch M, Gorski DJ, Abrams M, Piroth M, Schneckmann R, Homann S, Muller J, Hartwig S, Lehr S, et al. Cardiac Hyaluronan Synthesis Is Critically Involved in the Cardiac Macrophage Response and Promotes Healing After Ischemia Reperfusion Injury. Circ Res. 2019; 124:1433–1447. [PubMed: 30916618]
17. Fraccarollo D, Thomas S, Scholz CJ, Hilfiker-Kleiner D, Galuppo P, Bauersachs J. Macrophage Mineralocorticoid Receptor Is a Pleiotropic Modulator of Myocardial Infarct Healing. Hypertension. 2019; 73:102–111. [PubMed: 30543467]
18. Howangyin KY, Zlatanova I, Pinto C, Ngkelo A, Cochain C, Rouanet M, Vilar J, Lemitre M, Stockmann C, Fleischmann BK, et al. Myeloid-Epithelial-Reproductive Receptor Tyrosine Kinase and Milk Fat Globule Epidermal Growth Factor 8 Coordinately Improve Remodeling After Myocardial Infarction via Local Delivery of Vascular Endothelial Growth Factor. Circulation. 2016; 133:826–839. [PubMed: 26819373]
19. Wu X, Reboll MR, Korf-Klingebiel M, Wollert KC. Angiogenesis after acute myocardial infarction. Cardiovasc Res. 2021; 117:1257–1273. [PubMed: 33063086]
20. Wong NR, Mohan J, Kopecky BJ, Guo S, Du L, Leid J, Feng G, Lokshina I, Dmytrenko O, Luehmann H, et al. Resident cardiac macrophages mediate adaptive myocardial remodeling. Immunity. 2021; 54:2072–2088 e2077. [PubMed: 34320366]
21. Batlle E, Massague J. Transforming Growth Factor-beta Signaling in Immunity and Cancer. Immunity. 2019; 50:924–940. [PubMed: 30995507]
22. Sanjabi S, Oh SA, Li MO. Regulation of the Immune Response by TGF-beta: From Conception to Autoimmunity and Infection. Cold Spring Harb Perspect Biol. 2017; 9.
23. Frangogiannis NG. The role of transforming growth factor (TGF)-beta in the infarcted myocardium. J Thorac Dis. 2017; 9:S52–S63. [PubMed: 28446968]
24. Frangogiannis NG. Transforming growth factor-beta in myocardial disease. Nat Rev Cardiol. 2022:doi: 10.1038/s41569-41021-00646-w. Online ahead of print.
25. Wahl SM, Hunt DA, Wakefield LM, McCartney-Francis N, Wahl LM, Roberts AB, Sporn MB. Transforming growth factor type beta induces monocyte chemotaxis and growth factor production. Proc Natl Acad Sci U S A. 1987; 84:5788–5792. [PubMed: 2886992]
26. Wiseman DM, Polverini PJ, Kamp DW, Leibovich SJ. Transforming growth factor-beta (TGF beta) is chemotactic for human monocytes and induces their expression of angiogenic activity. Biochem Biophys Res Commun. 1988; 157:793–800. [PubMed: 2462419]
27. Wahl SM, Allen JB, Weeks BS, Wong HL, Klotman PE. Transforming growth factor beta enhances integrin expression and type IV collagenase secretion in human monocytes. Proc Natl Acad Sci U S A. 1993; 90:4577–4581. [PubMed: 8506302]
28. Xiao YQ, Freire-de-Lima CG, Janssen WJ, Morimoto K, Lyu D, Bratton DL, Henson PM. Oxidants selectively reverse TGF-beta suppression of proinflammatory mediator production. J Immunol. 2006; 176:1209–1217. [PubMed: 16394011]
29. McDonald PP, Fadok VA, Bratton D, Henson PM. Transcriptional and translational regulation of inflammatory mediator production by endogenous TGF-beta in macrophages that have ingested apoptotic cells. J Immunol. 1999; 163:6164–6172. [PubMed: 10570307]
30. Kitamura M. Identification of an inhibitor targeting macrophage production of monocyte chemoattractant protein-1 as TGF-beta 1. J Immunol. 1997; 159:1404–1411. [PubMed: 9233637]
31. Nakao A, Afrakhte M, Moren A, Nakayama T, Christian JL, Heuchel R, Itoh S, Kawabata M, Heldin NE, Heldin CH, et al. Identification of Smad7, a TGFbeta-inducible antagonist of TGF-beta signalling. Nature. 1997; 389:631–635. [PubMed: 9335507]
32. Humeres C, Shinde AV, Hanna A, Alex L, Hernandez SC, Li R, Chen B, Conway SJ, Frangogiannis NG. Smad7 effects on TGF-beta and ErbB2 restrain myofibroblast activation and

protect from postinfarction heart failure. J Clin Invest. 2022; 132:e146926. doi: 146910.141172/JCI146926. [PubMed: 34905511]

33. Hong S, Lim S, Li AG, Lee C, Lee YS, Lee EK, Park SH, Wang XJ, Kim SJ. Smad7 binds to the adaptors TAB2 and TAB3 to block recruitment of the kinase TAK1 to the adaptor TRAF2. Nat Immunol. 2007; 8:504–513. [PubMed: 17384642]
34. Wang W, Huang XR, Li AG, Liu F, Li JH, Truong LD, Wang XJ, Lan HY. Signaling mechanism of TGF-beta1 in prevention of renal inflammation: role of Smad7. J Am Soc Nephrol. 2005; 16:1371–1383. [PubMed: 15788474]
35. Monteleone G, Mann J, Monteleone I, Vavassori P, Bremner R, Fantini M, Del Vecchio Blanco G, Tersigni R, Alessandroni L, Mann D, et al. A failure of transforming growth factor-beta1 negative regulation maintains sustained NF-kappaB activation in gut inflammation. J Biol Chem. 2004; 279:3925–3932. [PubMed: 14600158]
36. Monteleone G, Pallone F, MacDonald TT. Smad7 in TGF-beta-mediated negative regulation of gut inflammation. Trends Immunol. 2004; 25:513–517. [PubMed: 15364052]
37. Kleiter I, Song J, Lukas D, Hasan M, Neumann B, Croxford AL, Pedre X, Hovelmeyer N, Yogev N, Mildner A, et al. Smad7 in T cells drives T helper 1 responses in multiple sclerosis and experimental autoimmune encephalomyelitis. Brain. 2010; 133:1067–1081. [PubMed: 20354004]
38. Sasmono RT, Oceandy D, Pollard JW, Tong W, Pavli P, Wainwright BJ, Ostrowski MC, Himes SR, Hume DA. A macrophage colony-stimulating factor receptor-green fluorescent protein transgene is expressed throughout the mononuclear phagocyte system of the mouse. Blood. 2003; 101:1155–1163. [PubMed: 12393599]
39. Hayashi S, McMahon AP. Efficient recombination in diverse tissues by a tamoxifen-inducible form of Cre: a tool for temporally regulated gene activation/inactivation in the mouse. Dev Biol. 2002; 244:305–318. [PubMed: 11944939]
40. Huang S, Chen B, Su Y, Alex L, Humeres C, Shinde AV, Conway SJ, Frangogiannis NG. Distinct roles of myofibroblast-specific Smad2 and Smad3 signaling in repair and remodeling of the infarcted heart. J Mol Cell Cardiol. 2019; 132:84–97. [PubMed: 31085202]
41. Shinde AV, Humeres C, Frangogiannis NG. The role of alpha-smooth muscle actin in fibroblast-mediated matrix contraction and remodeling. Biochim Biophys Acta. 2017; 1863:298–309.
42. Frunza O, Russo I, Saxena A, Shinde AV, Humeres C, Hanif W, Rai V, Su Y, Frangogiannis NG. Myocardial Galectin-3 Expression Is Associated with Remodeling of the Pressure-Overloaded Heart and May Delay the Hypertrophic Response without Affecting Survival, Dysfunction, and Cardiac Fibrosis. Am J Pathol. 2016; 186:1114–1127. [PubMed: 26948424]
43. Chen B, Li R, Kubota A, Alex L, Frangogiannis NG. Identification of macrophages in normal and injured mouse tissues using reporter lines and antibodies. Sci Rep. 2022; 12:4542. [PubMed: 35296717]
44. Trapnell C, Pachter L, Salzberg SL. TopHat: discovering splice junctions with RNA-Seq. Bioinformatics. 2009; 25:1105–1111. [PubMed: 19289445]
45. Trapnell C, Williams BA, Pertea G, Mortazavi A, Kwan G, van Baren MJ, Salzberg SL, Wold BJ, Pachter L. Transcript assembly and quantification by RNA-Seq reveals unannotated transcripts and isoform switching during cell differentiation. Nat Biotechnol. 2010; 28:511–515. [PubMed: 20436464]
46. Anders S, Pyl PT, Huber W. HTSeq--a Python framework to work with high-throughput sequencing data. Bioinformatics. 2015; 31:166–169. [PubMed: 25260700]
47. Anders S, Huber W. Differential expression analysis for sequence count data. Genome Biol. 2010; 11:R106. [PubMed: 20979621]
48. Bronzert DA, Bates SE, Sheridan JP, Lindsey R, Valverius EM, Stampfer MR, Lippman ME, Dickson RB. Transforming growth factor-beta induces platelet-derived growth factor (PDGF) messenger RNA and PDGF secretion while inhibiting growth in normal human mammary epithelial cells. Mol Endocrinol. 1990; 4:981–989. [PubMed: 2178225]
49. Takaishi T, Matsui T, Tsukamoto T, Ito M, Taniguchi T, Fukase M, Chihara K. TGF-beta-induced macrophage colony-stimulating factor gene expression in various mesenchymal cell lines. Am J Physiol. 1994; 267:C25–31. [PubMed: 8048485]

50. Gal-Oz ST, Maier B, Yoshida H, Seddu K, Elbaz N, Czysz C, Zuk O, Stranger BE, Ner-Gaon H, Shay T. ImmGen report: sexual dimorphism in the immune system transcriptome. Nature communications. 2019; 10:4295.
51. Gronroos E, Hellman U, Heldin CH, Ericsson J. Control of Smad7 stability by competition between acetylation and ubiquitination. Mol Cell. 2002; 10:483–493. [PubMed: 12408818]
52. Hanna A, Shinde AV, Frangogiannis NG. Validation of diagnostic criteria and histopathological characterization of cardiac rupture in the mouse model of nonreperfused myocardial infarction. Am J Physiol Heart Circ Physiol. 2020; 319:H948–H964. [PubMed: 32886000]
53. Zhang S, Bories G, Lantz C, Emmons R, Becker A, Liu E, Abecassis MM, Yvan-Charvet L, Thorp EB. Immunometabolism of Phagocytes and Relationships to Cardiac Repair. Front Cardiovasc Med. 2019; 6:42. [PubMed: 31032261]
54. Ma Y, Mouton AJ, Lindsey ML. Cardiac macrophage biology in the steady-state heart, the aging heart, and following myocardial infarction. Transl Res. 2018; 191:15–28. [PubMed: 29106912]
55. Mouton AJ, DeLeon-Pennell KY, Rivera Gonzalez OJ, Flynn ER, Freeman TC, Saucerman JJ, Garrett MR, Ma Y, Harmancey R, Lindsey ML. Mapping macrophage polarization over the myocardial infarction time continuum. Basic Res Cardiol. 2018; 113:26. [PubMed: 29868933]
56. Bajpai G, Bredemeyer A, Li W, Zaitsev K, Koenig AL, Lokshina I, Mohan J, Ivey B, Hsiao HM, Weinheimer C, et al. Tissue Resident CCR2− and CCR2+ Cardiac Macrophages Differentially Orchestrate Monocyte Recruitment and Fate Specification Following Myocardial Injury. Circ Res. 2019; 124:263–278. [PubMed: 30582448]
57. Frangogiannis NG, Mendoza LH, Lindsey ML, Ballantyne CM, Michael LH, Smith CW, Entman ML. IL-10 is induced in the reperfused myocardium and may modulate the reaction to injury. J Immunol. 2000; 165:2798–2808. [PubMed: 10946312]
58. Murry CE, Giachelli CM, Schwartz SM, Vracko R. Macrophages express osteopontin during repair of myocardial necrosis. Am J Pathol. 1994; 145:1450–1462. [PubMed: 7992848]
59. Shirakawa K, Endo J, Kataoka M, Katsumata Y, Anzai A, Moriyama H, Kitakata H, Hiraide T, Ko S, Goto S, et al. MerTK Expression and ERK Activation Are Essential for the Functional Maturation of Osteopontin-Producing Reparative Macrophages After Myocardial Infarction. J Am Heart Assoc. 2020; 9:e017071. [PubMed: 32865099]
60. Shiraishi M, Shintani Y, Shintani Y, Ishida H, Saba R, Yamaguchi A, Adachi H, Yashiro K, Suzuki K. Alternatively activated macrophages determine repair of the infarcted adult murine heart. J Clin Invest. 2016; 126:2151–2166. [PubMed: 27140396]
61. Reboll MR, Korf-Klingebiel M, Klede S, Polten F, Brinkmann E, Reimann I, Schonfeld HJ, Bobadilla M, Faix J, Kensah G, et al. EMC10 (Endoplasmic Reticulum Membrane Protein Complex Subunit 10) Is a Bone Marrow-Derived Angiogenic Growth Factor Promoting Tissue Repair After Myocardial Infarction. Circulation. 2017; 136:1809–1823. [PubMed: 28931551]
62. Allen JB, Manthey CL, Hand AR, Ohura K, Ellingsworth L, Wahl SM. Rapid onset synovial inflammation and hyperplasia induced by transforming growth factor beta. J Exp Med. 1990; 171:231–247. [PubMed: 2295877]
63. Comalada M, Cardo M, Xaus J, Valledor AF, Lloberas J, Ventura F, Celada A. Decorin reverses the repressive effect of autocrine-produced TGF-beta on mouse macrophage activation. J Immunol. 2003; 170:4450–4456. [PubMed: 12707320]
64. Naiki Y, Michelsen KS, Zhang W, Chen S, Doherty TM, Arditi M. Transforming growth factor-beta differentially inhibits MyD88-dependent, but not TRAM- and TRIF-dependent, lipopolysaccharide-induced TLR4 signaling. J Biol Chem. 2005; 280:5491–5495. [PubMed: 15623538]
65. Rose DM, Fadok VA, Riches DW, Clay KL, Henson PM. Autocrine/paracrine involvement of platelet-activating factor and transforming growth factor-beta in the induction of phosphatidylserine recognition by murine macrophages. J Immunol. 1995; 155:5819–5825. [PubMed: 7499871]
66. Nurgazieva D, Mickley A, Moganti K, Ming W, Ovsyi I, Popova A, Sachindra, Awad K, Wang N, Bieback K, et al. TGF-beta1, but not bone morphogenetic proteins, activates Smad1/5 pathway in primary human macrophages and induces expression of proatherogenic genes. J Immunol. 2015; 194:709–718. [PubMed: 25505291]

67. Hong YH, Peng HB, La Fata V, Liao JK. Hydrogen peroxide-mediated transcriptional induction of macrophage colony-stimulating factor by TGF-beta1. J Immunol. 1997; 159:2418–2423. [PubMed: 9278333]

68. Celada A, Maki RA. Transforming growth factor-beta enhances the M-CSF and GM-CSF-stimulated proliferation of macrophages. J Immunol. 1992; 148:1102–1105. [PubMed: 1737928]

69. Boutard V, Havouis R, Fouqueray B, Philippe C, Moulinoux JP, Baud L. Transforming growth factor-beta stimulates arginase activity in macrophages. Implications for the regulation of macrophage cytotoxicity. J Immunol. 1995; 155:2077–2084. [PubMed: 7636258]

70. Xie B, Dong Z, Fidler IJ. Regulatory mechanisms for the expression of type IV collagenases/gelatinases in murine macrophages. J Immunol. 1994; 152:3637–3644. [PubMed: 8144939]

71. Werner F, Jain MK, Feinberg MW, Sibinga NE, Pellacani A, Wiesel P, Chin MT, Topper JN, Perrella MA, Lee ME. Transforming growth factor-beta 1 inhibition of macrophage activation is mediated via Smad3. J Biol Chem. 2000; 275:36653–36658. [PubMed: 10973958]

72. Feinberg MW, Jain MK, Werner F, Sibinga NE, Wiesel P, Wang H, Topper JN, Perrella MA, Lee ME. Transforming growth factor-beta 1 inhibits cytokine-mediated induction of human metalloelastase in macrophages. J Biol Chem. 2000; 275:25766–25773. [PubMed: 10825169]

73. Mojsilovic SS, Santibanez JF. Transforming growth factor-beta differently regulates urokinase type plasminogen activator and matrix metalloproteinase-9 expression in mouse macrophages; analysis of intracellular signal transduction. Cell Biol Int. 2015; 39:619–628. [PubMed: 25597879]

74. Jeon SH, Chae BC, Kim HA, Seo GY, Seo DW, Chun GT, Kim NS, Yie SW, Byeon WH, Eom SH, et al. Mechanisms underlying TGF-beta1-induced expression of VEGF and Flk-1 in mouse macrophages and their implications for angiogenesis. J Leukoc Biol. 2007; 81:557–566. [PubMed: 17053163]

75. de Ceuninck van Capelle C, Spit M, Ten Dijke P. Current perspectives on inhibitory SMAD7 in health and disease. Crit Rev Biochem Mol Biol. 2020; 55:691–715. [PubMed: 33081543]

76. Kamiya Y, Miyazono K, Miyazawa K. Smad7 inhibits transforming growth factor-beta family type i receptors through two distinct modes of interaction. J Biol Chem. 2010; 285:30804–30813. [PubMed: 20663871]

77. Humeres C, Shinde AV, Hanna A, Alex L, Hernandez SC, Li R, Chen B, Conway SJ, Frangogiannis NG. Smad7 effects on TGF-beta and Erbb2 restrain myofibroblast activation, and protect from post-infarction heart failure. J Clin Invest. 2021; e146926. doi: 10.1172/JCI146926. Online ahead of print.

78. Dennis EA, Smythies LE, Grabski R, Li M, Ballestas ME, Shimamura M, Sun JJ, Grams J, Stahl R, Niederweis ME, et al. Cytomegalovirus promotes intestinal macrophage-mediated mucosal inflammation through induction of Smad7. Mucosal Immunol. 2018; 11:1694–1704. [PubMed: 30076393]

79. Nie J, Hao W, Dou X, Wang X, Luo N, Lan HY, Yu X. Effects of Smad7 overexpression on peritoneal inflammation in a rat peritoneal dialysis model. Perit Dial Int. 2007; 27:580–588. [PubMed: 17704451]

80. Saika S, Ikeda K, Yamanaka O, Miyamoto T, Ohnishi Y, Sato M, Muragaki Y, Ooshima A, Nakajima Y, Kao WW, et al. Expression of Smad7 in mouse eyes accelerates healing of corneal tissue after exposure to alkali. Am J Pathol. 2005; 166:1405–1418. [PubMed: 15855641]

81. Imhof BA, Ballet R, Hammel P, Jemelin S, Garrido-Urbani S, Ikeya M, Matthes T, Miljkovic-Licina M. Olfactomedin-like 3 promotes PDGF-dependent pericyte proliferation and migration during embryonic blood vessel formation. FASEB J. 2020; 34:15559–15576. [PubMed: 32997357]

82. Miljkovic-Licina M, Hammel P, Garrido-Urbani S, Lee BP, Meguenani M, Chaabane C, Bochaton-Piallat ML, Imhof BA. Targeting olfactomedin-like 3 inhibits tumor growth by impairing angiogenesis and pericyte coverage. Mol Cancer Ther. 2012; 11:2588–2599. [PubMed: 23002094]

83. Boufenzer A, Lemarie J, Simon T, Derive M, Bouazza Y, Tran N, Maskali F, Groubatch F, Bonnin P, Bastien C, et al. TREM-1 Mediates Inflammatory Injury and Cardiac Remodeling Following Myocardial Infarction. Circ Res. 2015; 116:1772–1782. [PubMed: 25840803]

84. Lemarie J, Boufenzer A, Popovic B, Tran N, Groubatch F, Derive M, Labroca P, Barraud D, Gibot S. Pharmacological inhibition of the triggering receptor expressed on myeloid cells-1 limits

reperfusion injury in a porcine model of myocardial infarction. ESC Heart Fail. 2015; 2:90–99. [PubMed: 28834656]

85. Rienks M, Carai P, Bitsch N, Schellings M, Vanhaverbeke M, Verjans J, Cuijpers I, Heymans S, Papageorgiou A. Sema3A promotes the resolution of cardiac inflammation after myocardial infarction. Basic Res Cardiol. 2017; 112:42. [PubMed: 28540528]

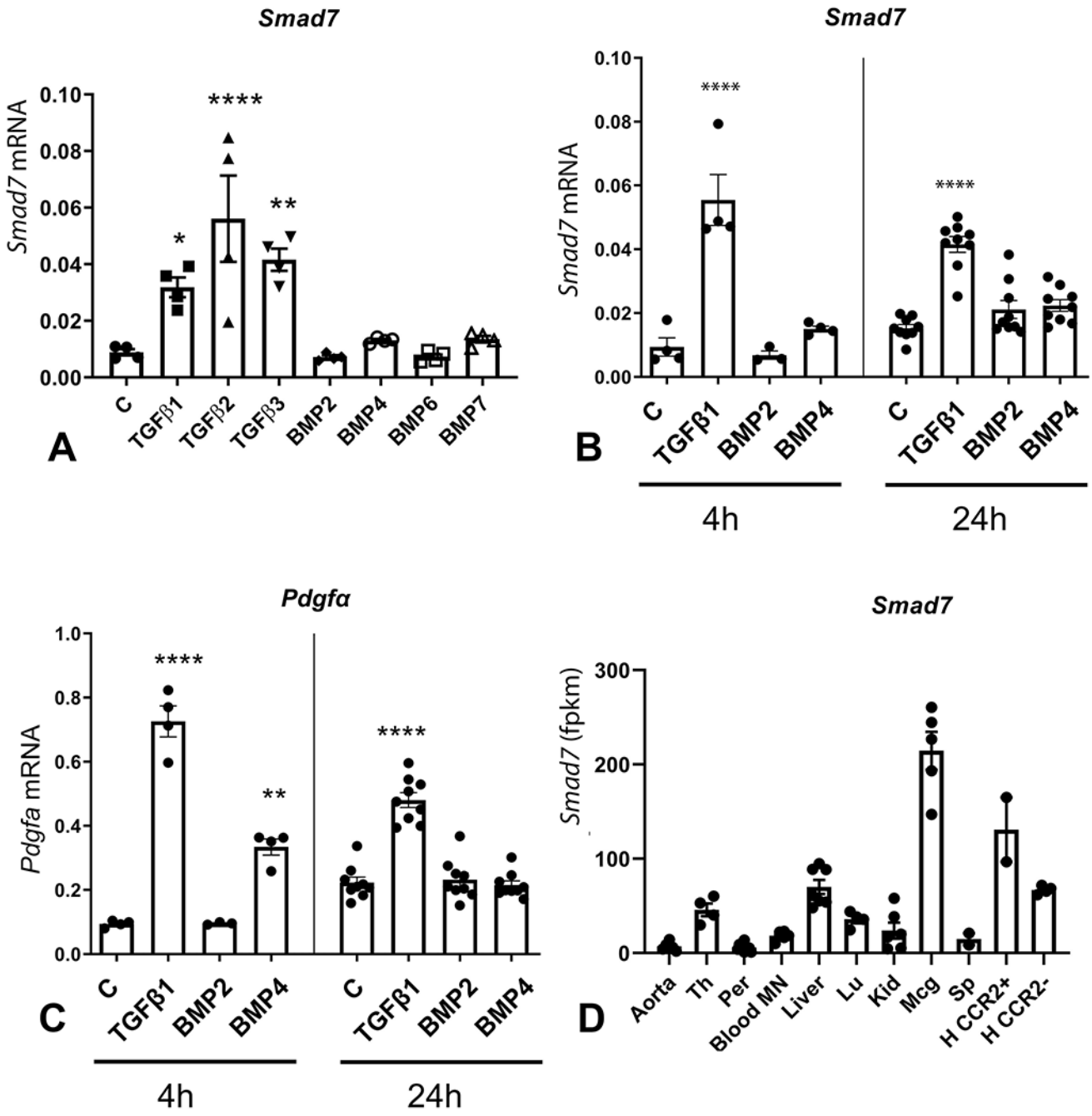

Figure 1: Smad7 expression in macrophages in vitro and in vivo.

A: TGF-β1, -β2 and -β3 (10ng/ml) markedly induced Smad7 mRNA expression in bone marrow macrophages (BMMs) after 4h of stimulation. In contrast, BMP2, BMP4, BMP6 and BMP7 (50ng/ml) have no significant effects (*p<0.05, **p<0.01, ****p<0.0001 vs. control; n=4/group). B: After 24h of stimulation, TGF-β1, but not BMP2 and BMP4 induced *Smad7* upregulation in BMMs. C: In contrast, *Pdgfa*, a gene induced by TGF-β superfamily members in several different cell types was upregulated in BMMs in response to TGF-β1, or BMP4 stimulation (4h experiment). In the prolonged stimulation experiment (24h) only

TGF-β1 increased *Pdgfa* expression levels (**p<0.01, ****p<0.0001, n=. n=3-4 for 4h stimulation, n=7-8 for the 24h stimulation experiment). D**: Smad7 expression patterns in mouse macrophages from different organs obtained by analyzing data from the Immgen database.** Microglial (Mcg) macrophages exhibit the highest levels of Smad7 expression, followed by $CCR2^{+}$ and $CCR2^{-}$ cardiac macrophages (H CCR2+ and H CCR2− respectively), liver, and thymus (Th) macrophages. In contrast, aortic, peritoneal (Per), renal (Kid), spleen macrophages (Sp), and circulating blood monocytes (blood MN) have low baseline levels of Smad7 expression.

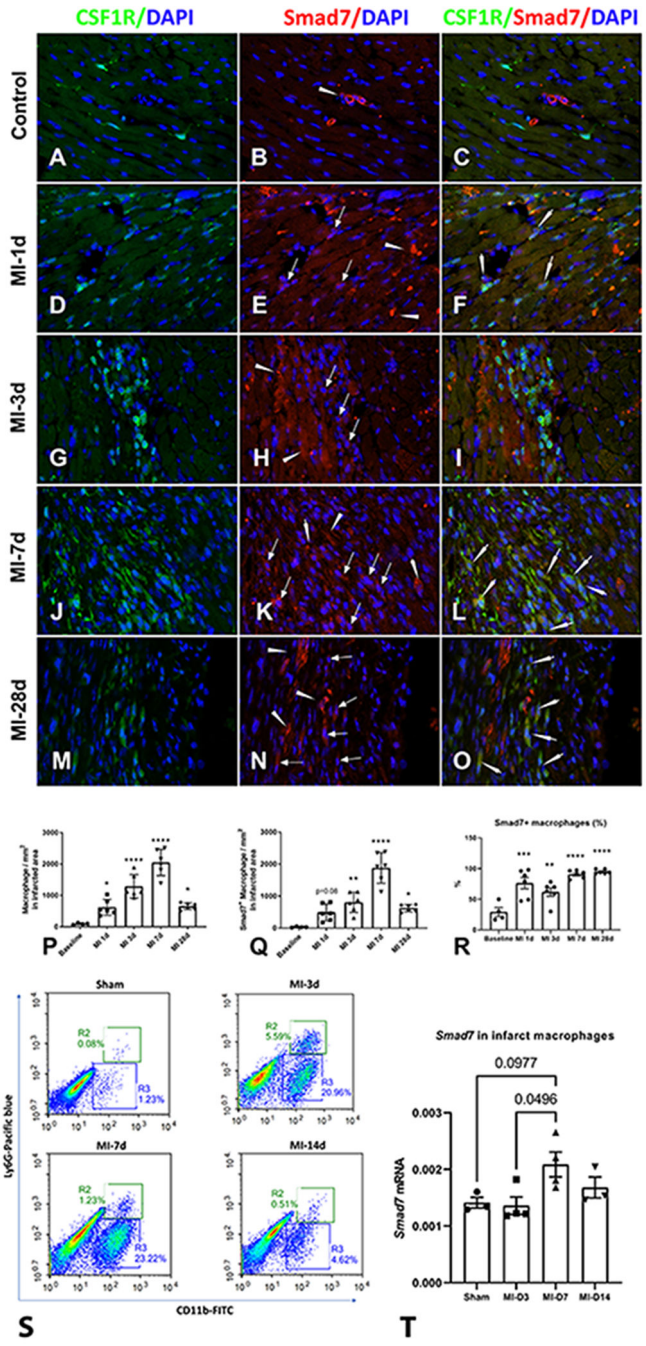

Figure 2: Time course of macrophage Smad7 expression in the infarcted myocardium.

CSF1R^{EGFP} reporter mice underwent non-reperfused myocardial infarction. Dual immunofluorescent staining for Smad7 and GFP was used to identify SMAD7+ macrophages. A-C: Control mouse hearts have a small population of CSF1R+ myeloid cells (A), and SMAD 7+ cells (B, arrowhead). D-F: After 24h of myocardial infarction, a small population of SMAD7+/CSF1R+ myeloid cells is detected in the infarcted area (arrowheads). G-I: After 3 days of coronary occlusion, abundant CSF1R+ myeloid cells (G) and SMAD7+ cells (H, arrows) are identified in the infarcted myocardium. J-L: Numerous

SMAD7+/CSF1R+ macrophages (arrowheads) are identified in the infarcted area after 7 days of myocardial infarction. M-O: The density of SMAD7+ macrophages is reduced after 28 days of infarction. P: Quantitative analysis shows that the density of CSF1R+ macrophages in the infarcted myocardium significantly increases after 3 days and peaks after 7 days of myocardial infarction. Q: The number of SMAD7+ macrophages peaks at the 7-day timepoint. R: The fraction of SMAD7+ macrophages shows an early increase 24h after coronary occlusion and peaks after 7-28 days of coronary occlusion (*p<0.05, **p<0.01, ***p<0.001, ****p<0.0001 vs. Control; n=4-6/group). S: Flow cytometric sorting was used to harvest CD11b+/Ly6G− macrophages from sham wildtype hearts and from infarcts after 3, 7 and 14 days of coronary occlusion. T: qPCR showed a significant change in Smad7 levels in infarct macrophages (ANOVA, p=0.048, n=3-4/group). 7 days after coronary occlusion, infarct macrophages exhibited a ~50% increase in *Smad7* mRNA levels, when compared with 3-day macrophages (p=0.0496, Tukey post-hoc test, n=4/group), or with macrophages harvested from sham hearts (p=0.0977, Tukey correction, n=3-4/group). This observation suggests that the increase in the density of SMAD7+ macrophages in the infarct is, at least in part, related to *Smad7* upregulation.

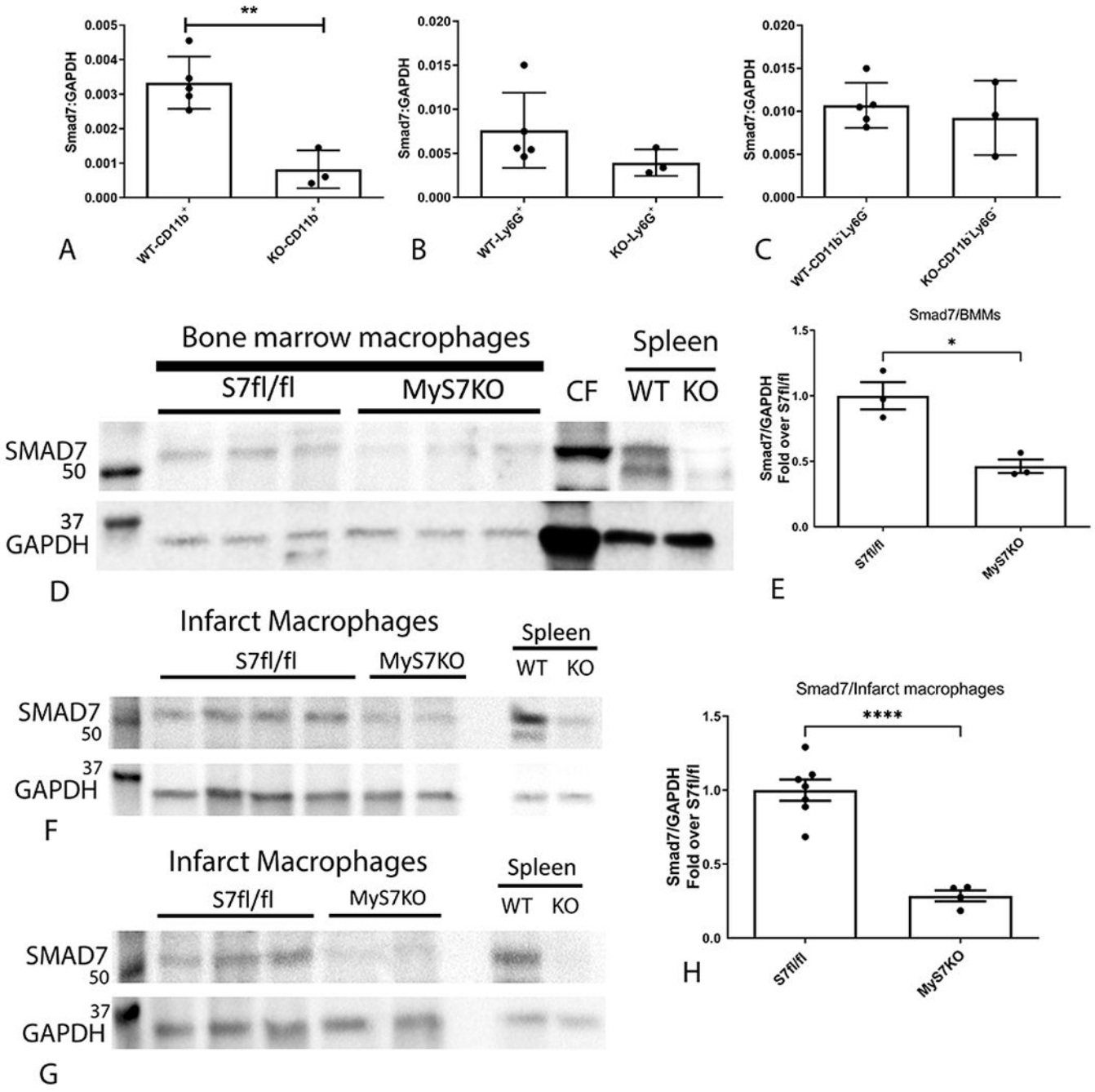

Figure 3: Documentation of Smad7 loss in myeloid cell-specific Smad7 KO (MyS7KO) mice.

Infarct macrophages harvested from MyS7KO infarcts exhibit a marked reduction in Smad7 mRNA and protein expression. CD11b+/Ly6G− macrophages, CD11b+/Ly6G+ neutrophils and CD11b−/Ly6G− non-myeloid interstitial cells were harvested from the infarcted heart of MyS7KO and Smad7 fl/fl mice after 3 days of permanent coronary occlusion. Macrophages (A), but not neutrophils (B) and non-myeloid interstitial cells (C) harvested from MyS7KO infarcts exhibit a marked decrease of *Smad7* expression, when compared to cells harvested from Smad7 fl/fl infarcts (**p<0.01 vs. Smad7 fl/fl; n=3-4/group). D-H: Western blotting

was performed to confirm macrophage SMAD7 loss in MyS7KO mice. Bone marrow macrophages (BMM) were harvested from Smad7 fl/fl and MyS7KO mice. Western blotting showed a marked reduction in SMAD7 levels in MyS7KO BMMs (*$p<0.05$, n=3/group) (D-E). Protein from TGF-β stimulated cardiac fibroblasts (CF)[32] serves as a positive control. Samples from the spleen of WT mouse and mouse with global inducible Smad7 knockout (KO) serves to validate the specificity of the antibody (please note that in tissue, a second SMAD7 band is noted right below the 50kDa marker). F-G: MyS7KO infarct macrophages also exhibit a reduction in SMAD7 levels. H: Quantitative analysis shows that MyS7KO infarct macrophages have markedly lower SMAD7 protein levels, when compared to infarct macrophages harvested from Smad7 fl/fl mice (5 days coronary occlusion, ****$p<0.0001$, n=4-7/group).

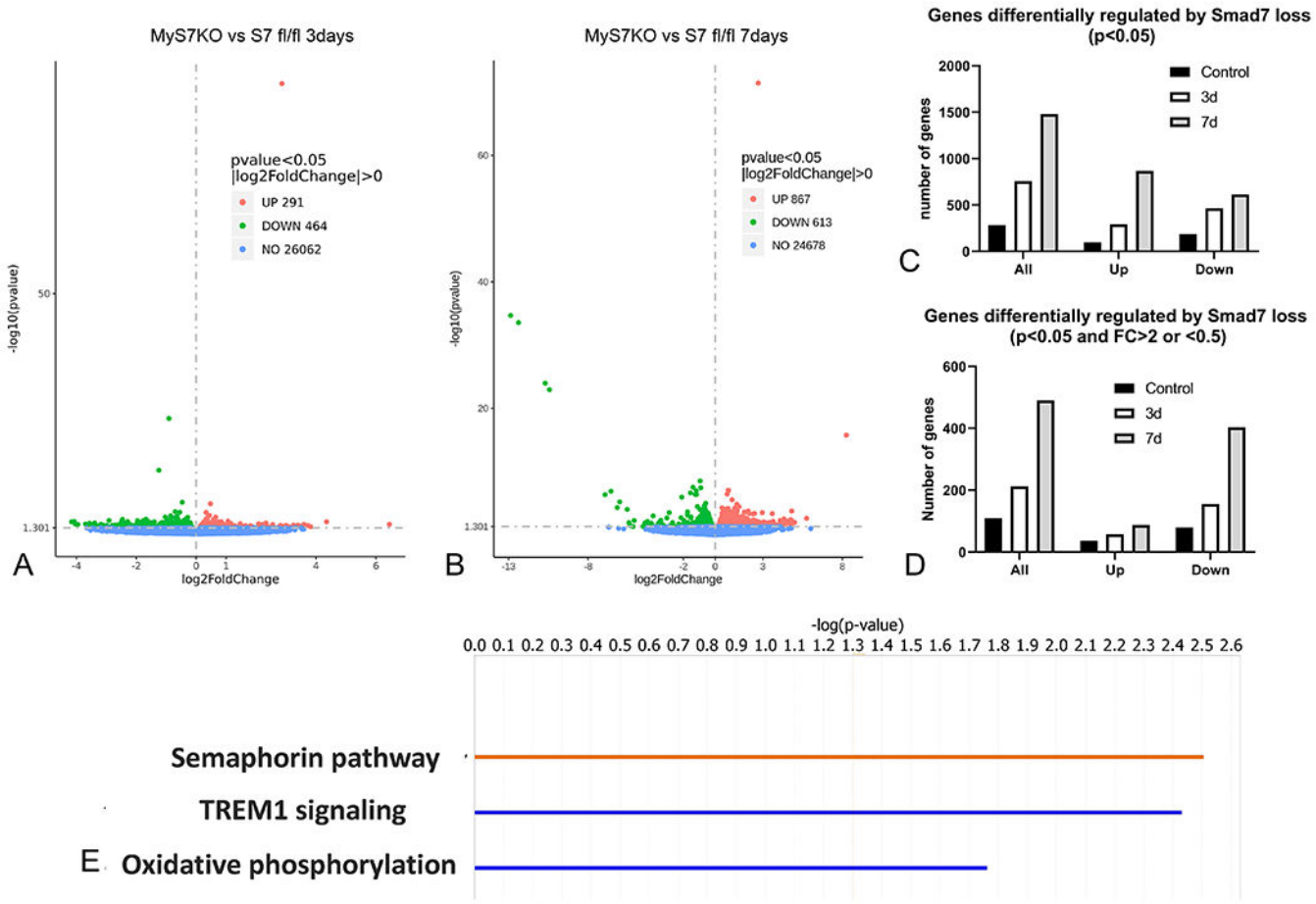

Figure 4: Effects of Myeloid cell-specific Smad7 loss on the gene expression profile of infarct macrophages.

A-D: RNA-seq was used to compare the transcriptional profile of infarct macrophages harvested from MyS7KO and Smad7 fl/fl infarcted hearts, 3 and 7 days after coronary occlusion. Volcano plots demonstrate upregulation of 291 genes and downregulation of 464 genes in Smad7 KO macrophages 3 days after myocardial infarction (A). 867 genes were upregulated and 613 genes were downmodulated by macrophage-specific loss of Smad7 at the 7-day post-infarction timepoint (B). C-D: the number of genes up and down regulated in MyS7KO infarct macrophages. E: Ingenuity pathway analysis (IPA) of the transcriptomic data at the 7-day timepoint identified 3 canonical pathways that were differentially regulated by Smad7 loss (with an absolute z score >2). The semaphorin pathway was predicted to be activated in Smad7 KO cells, whereas TREM1 signaling and oxidative phosphorylation were predicted to be inhibited.

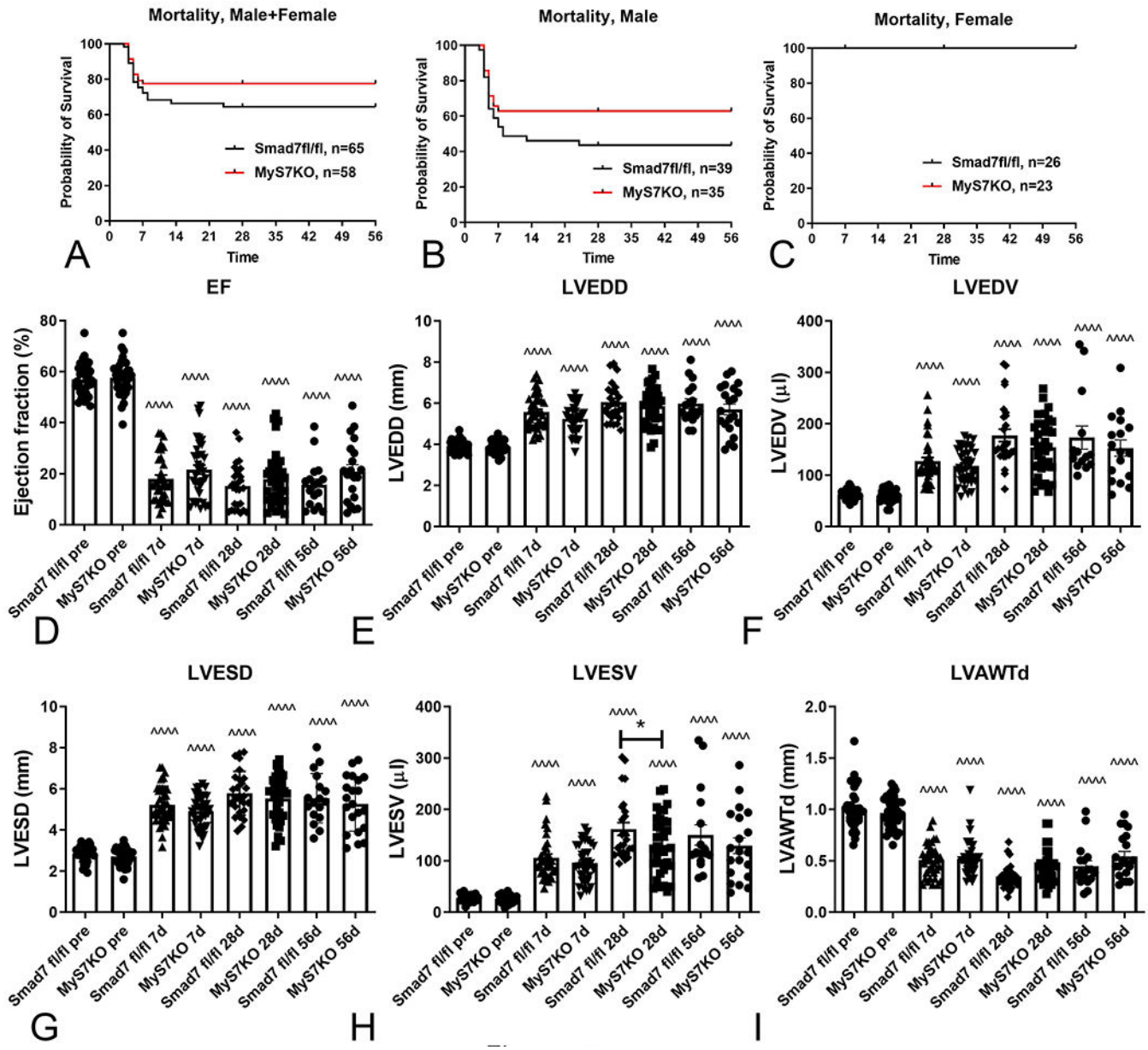

Figure 5: Myeloid cell-specific Smad7 loss does not affect mortality, dysfunction and adverse remodeling after myocardial infarction.

A-C: Male and female MyS7KO mice and corresponding sex-matched Smad7 fl/fl animals had comparable survival curves after myocardial infarction. B: Male mice exhibit marked mortality during the first week following infarction, that is not affected by myeloid cell-specific Smad7 loss (p=NS, Smad7 fl/fl, n=39; MyS7KO, n=35). C: All female mice survived permanent coronary occlusion surgery and no significant differences in mortality were noted (Smad7 fl/fl, n=26; MyS7KO, n=23). D-I: Post-infarction dysfunction and remodeling was studied using echocardiography 7, 28 and 56 days after infarction. MyS7KO and Smad7 fl/fl mice had comparable ejection fraction after 7, 28 and 56 days of coronary occlusion (D). E-G: Smad7 loss did not significantly affect LVEDD, LVEDV, and LVESD after 7-56 days of coronary occlusion. LVESV was modestly, but significantly lower in

MyS7KO mice at the 28-day timepoint; however, no significant effects of myeloid cell-specific Smad7 loss on LVESV were noted at the 7 and 56-day timepoints (H). Left ventricular anterior wall thickness was comparable between groups at all timepoints (I). (*p<0.05 vs smad7fl/fl 28d, ^^^^p<0.0001 vs corresponding pre-echo).

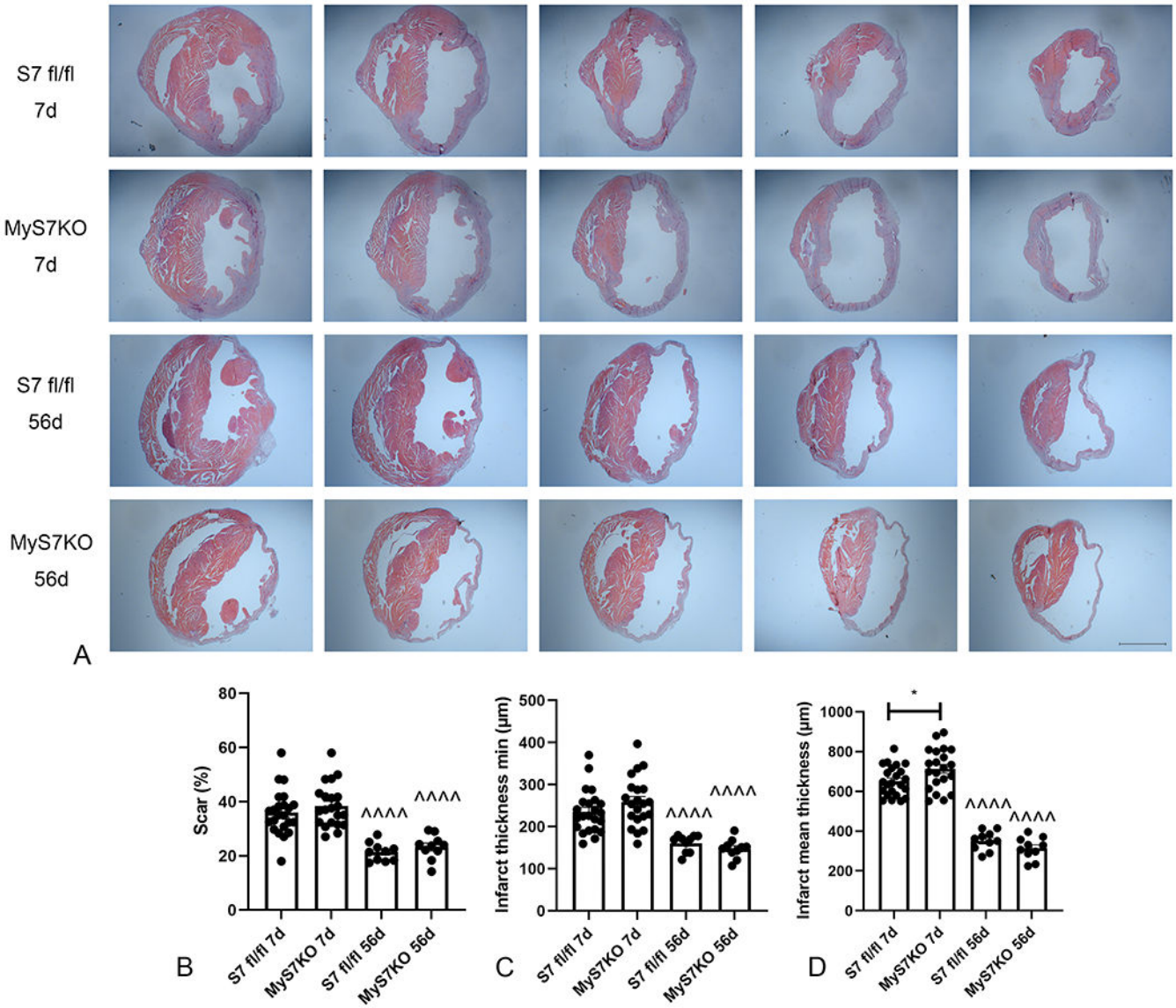

Figure 6: Myeloid cell-specific Smad7 loss does not affect scar size after myocardial infarction.

Effects of myeloid cell-specific Smad7 loss on scar size and remodeling 7 and 56 days after infarction were studied using systematic reconstruction of the entire infarcted ventricle by sectioning from base to apex (A). Scale bar=2mm. The scar size (B) and minimal thickness of the scar (C) were comparable between MyS7KO and Smad7 fl/fl groups at the 7 and 56-day post-infarction timepoints. D: Mean infarct thickness was modestly, but significantly higher in MyS7KO mice at the 7-day timepoint, however, no significant difference was noted between groups at 56-day timepoint following infarction. (*$p<0.05$ vs. Smad7fl/fl 7d, ^^^^$p<0.0001$ vs. corresponding 7d; n=10-23/group).

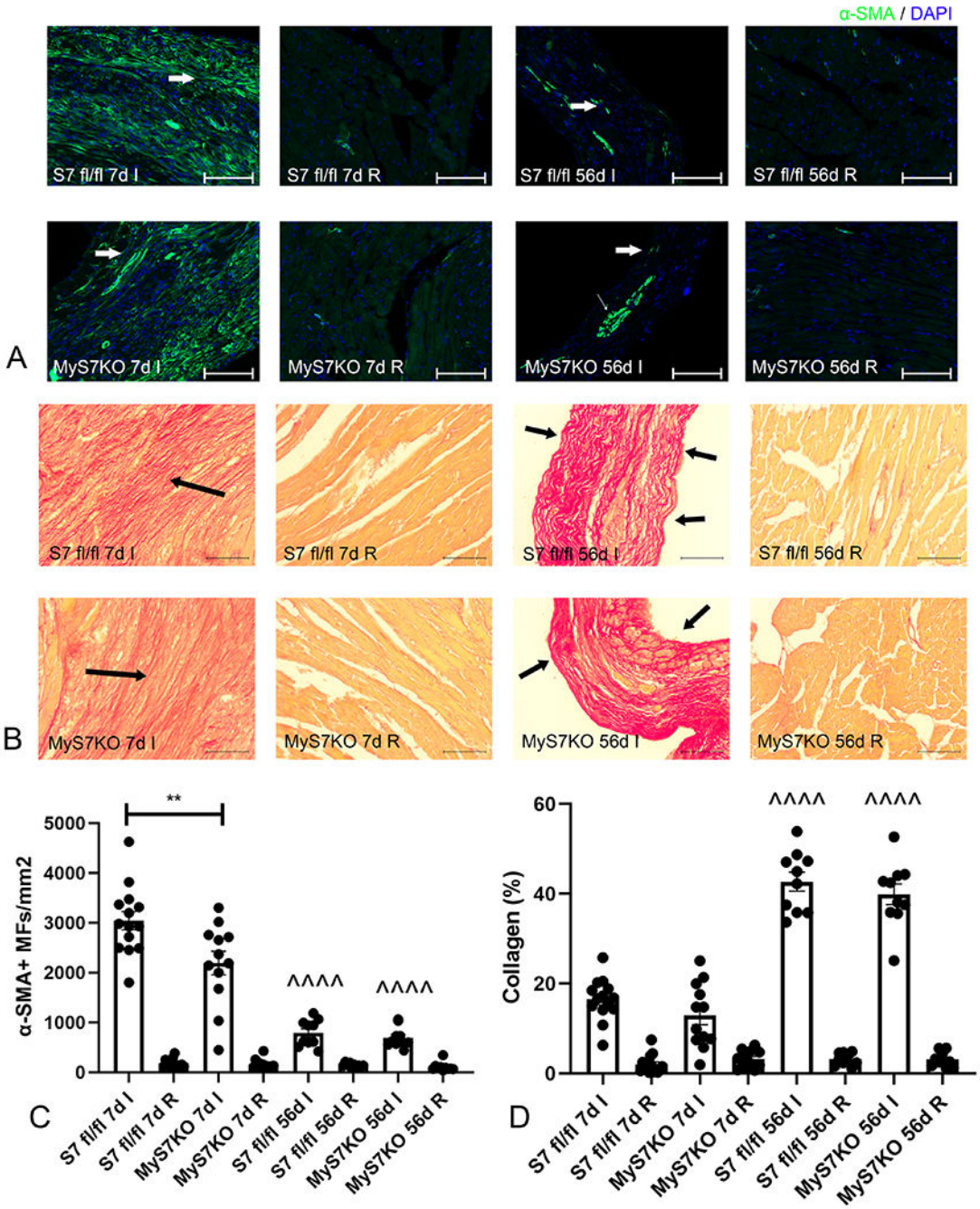

Figure 7: Myeloid cell-specific Smad7 loss transiently reduces myofibroblast density, but does not affect collagen deposition in the healing infarct.

A: Representative images identifying myofibroblasts, as α-smooth muscle actin (α-SMA)-immunoreactive cells located outside the media of vessels in the infarcted hearts. B: Picrosirius red staining was used to assess collagen content in the infarcted and remodeling myocardium. C: Myofibroblast density was modestly but significantly lower in MyS7KO infarcts, in comparison to Smad7 fl/fl infarcts at the 7-day timepoint. As the infarct scar matures, myofibroblast density markedly decreased and was comparable between groups at the 56-day timepoint. D: Quantitative analysis revealed no significant effects of myeloid

cell-specific Smad7 loss on collagen deposition in the infarct zone and in the remodeling myocardium at both timepoints examined. (**p<0.01 vs Smad7 fl/fl 7d, ^^^^p<0.0001 vs corresponding 7d; n=10-20/group).

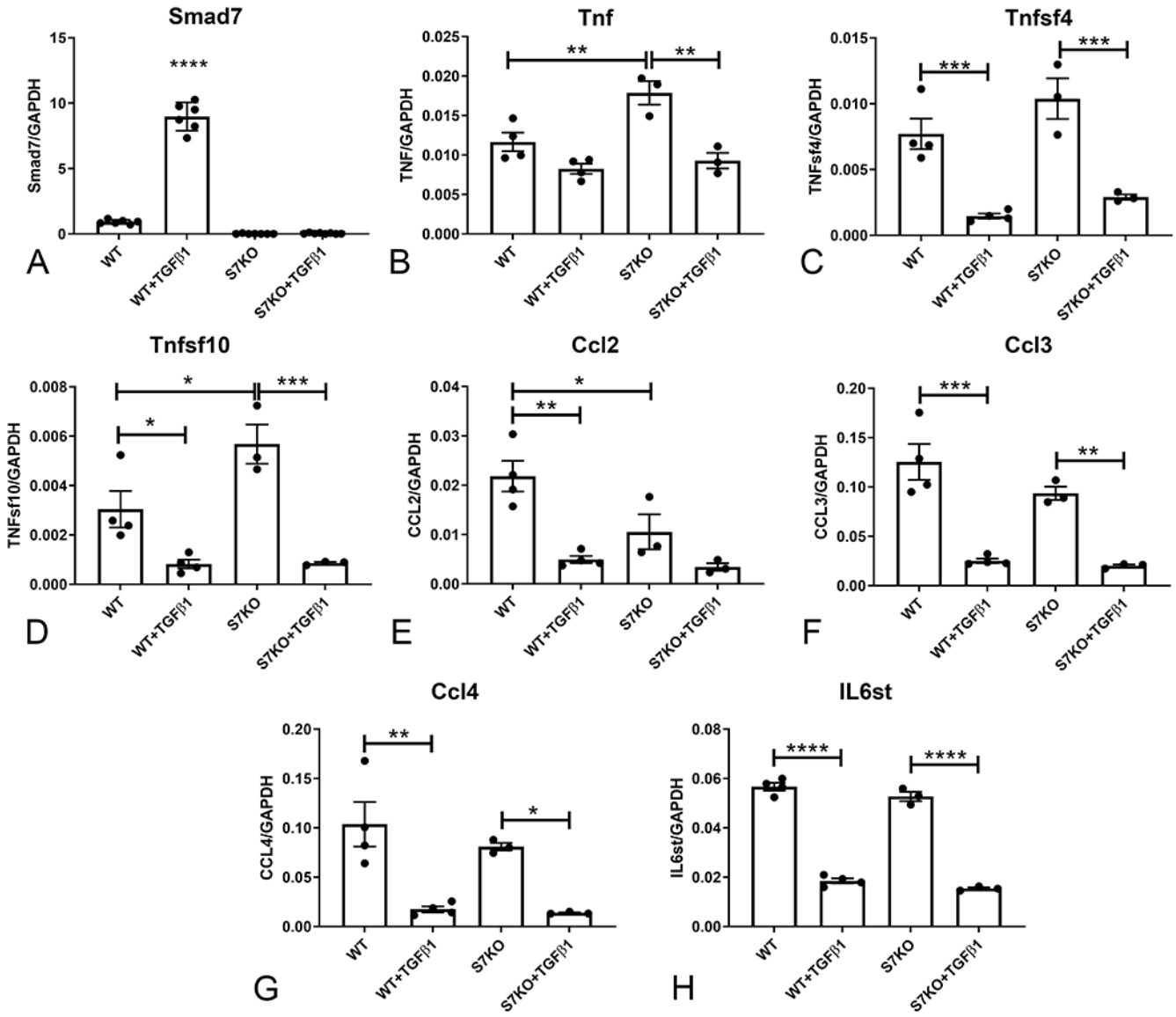

Figure 8: Effects of Smad7 loss on inflammatory genes expression in isolated bone marrow macrophages (BMM).

BMMs were stimulated with TGF-β1 (10ng/ml) for 4 hours. A: Loss of *Smad7* in Smad7 KO BMMs was confirmed by qPCR. B-H: Smad7 loss did not affect the anti-inflammatory actions of TGF-β1 on the expression of the inflammatory cytokines *Tnfa, Tnfsf4, Tnfsf10* (B-D), the chemokines *Ccl2, Ccl3, Ccl4* (E-G) and *Il6st* (H). Smad7 KO macrophages had higher baseline expression of *Tnfa* (B) and *Tnfsf10* (D), and lower baseline expression of *Ccl2* (E) (*p<0.05, **p<0.01, ***p<0.001, ****p<0.0001; n=3-4/group).

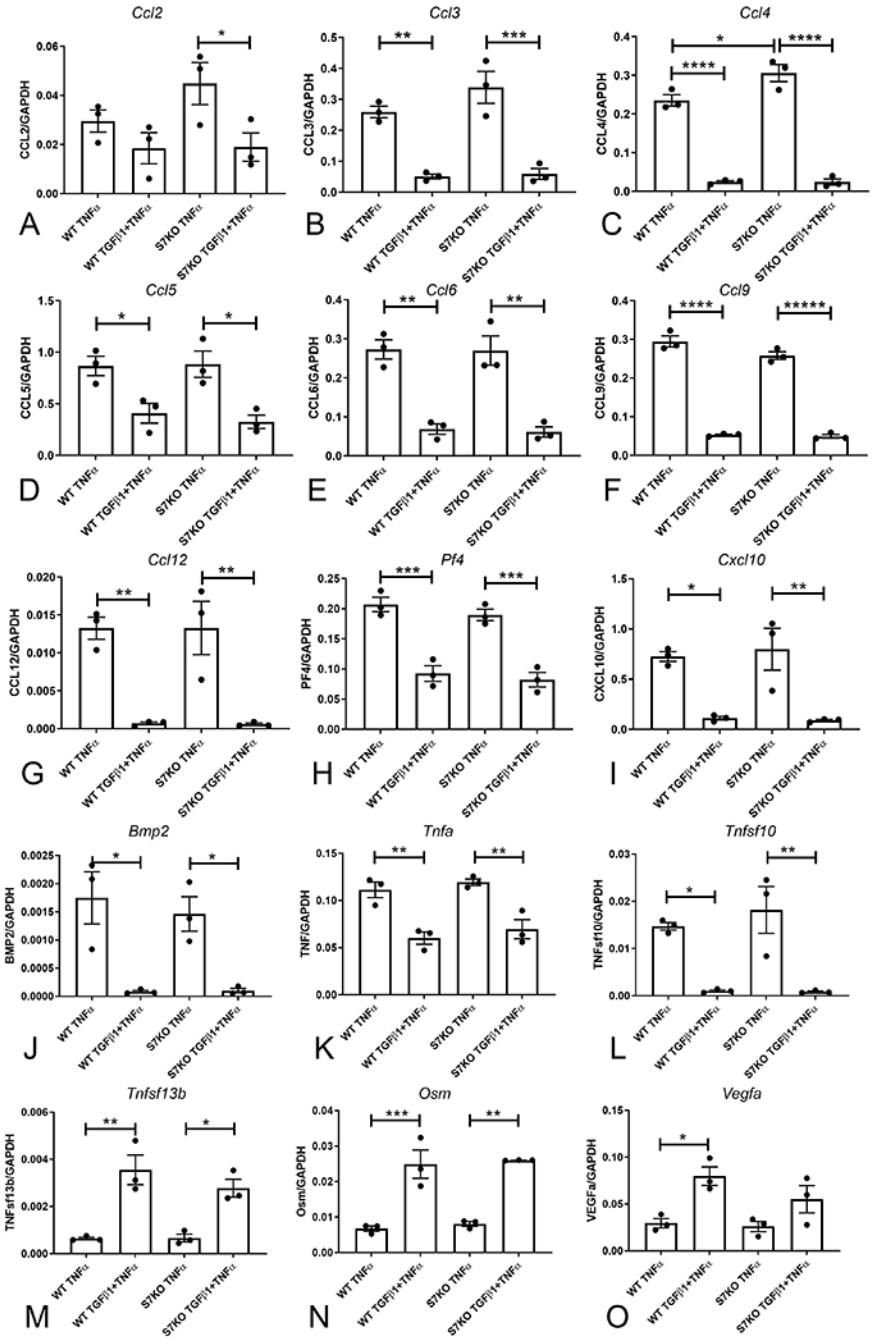

Figure 9: Smad7 loss does not affect the anti-inflammatory actions of TGF-β in TNF-α-stimulated bone marrow macrophages (BMMs).

WT (Smad7 fl/fl) and Smad7 KO BMMs were pre-treated with TGF-β1 (10ng/ml) for 2 hours, followed by stimulation with TNF-α (10ng/ml) for 4 hours. A-L: TGF-β1 markedly suppressed TNF-α induced inflammatory chemokine (*Ccl2, Ccl3, Ccl4, Ccl5, Ccl6, Ccl9, Ccl12, Pf4, Cxcl10*) and cytokine (*Bmp2, Tnfa, Tnfsf10*) gene expression in both WT and Smad7 KO cells. M-O: In contrast to its suppressive effects on expression of a wide range of pro-inflammatory cytokines, TGF-β1 upregulated synthesis of *Tnfsf13b, Osm* and *Vegfa*

in the presence of TNF-α. Smad7 absence did not affect these effects (*p<0.05, **p<0.01, ***p<0.001; n=3/group)

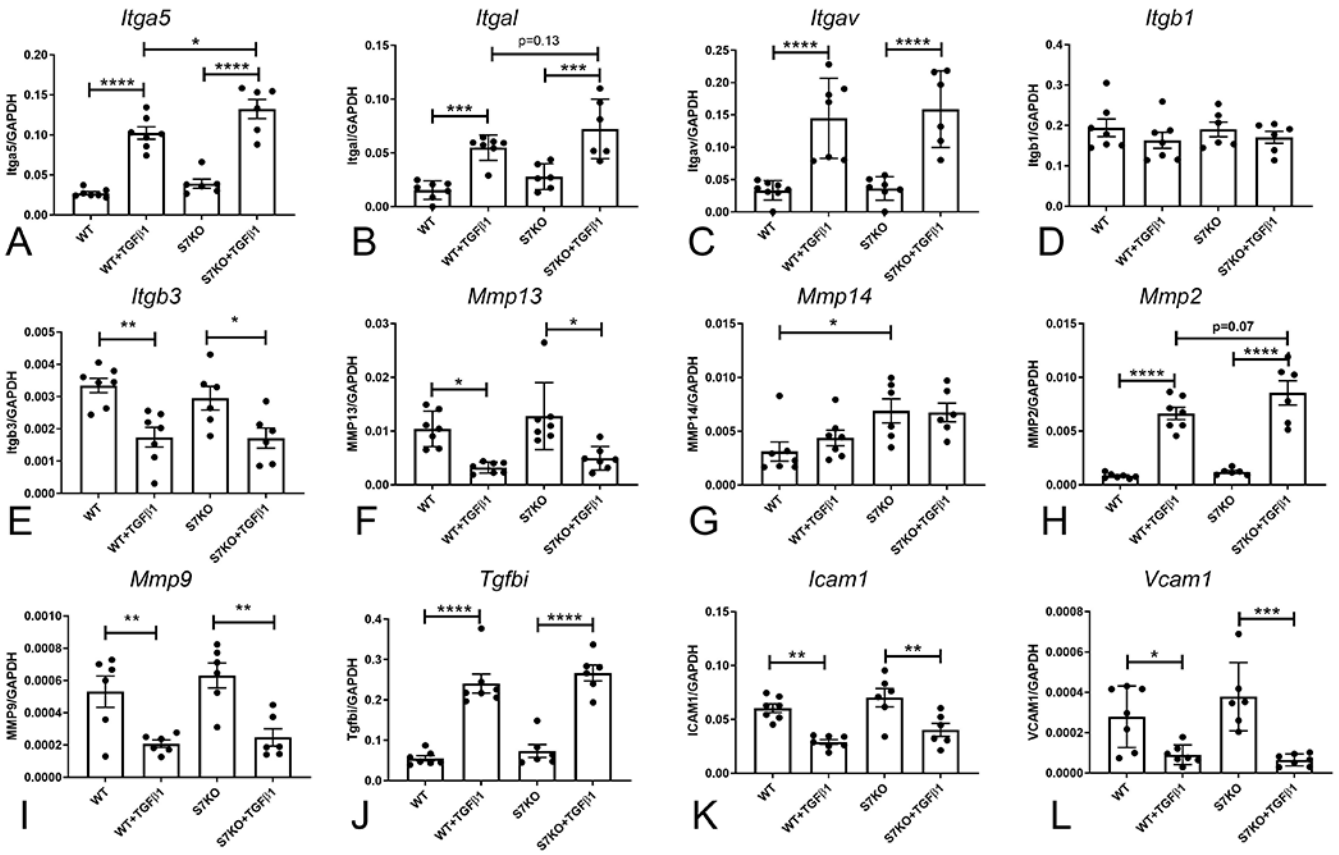

Figure 10: Effects of Smad7 loss on expression of matrix remodeling-associated genes in bone marrow macrophages (BMM).

TGF-β1 (10ng/ml) stimulation induced expression of integrins *Itga5, Itgal* and *Itgav* (A-C), had no significant effects on *Itgb1* levels (D) and downregulated *Itgb3* synthesis (E). Smad7 loss was associated with modest, but significant accentuation of TGF-β-induced *Itga5* expression (A). TGF-β1 suppressed *Mmp13* (F) and *Mmp9* (I) expression, markedly induced *Mmp2* (H) in both WT and Smad7 KO macrophages. Smad7 loss was associated with significantly increased baseline expression levels of *Mmp14* (G). TGF-β1 also markedly induced expression of the matricellular protein *Tgfbi* (J) and suppressed levels of the adhesion molecules *Icam1* (K) and *Vcam1* (L) in both WT and Smad7 KO cells. Smad7 loss did not affect expression levels of *Tgfbi, Vcam1* and *Icam1* in BMMs (J-L). (*p<0.05, **p<0.01, ***p<0.001; n=6-7/group).

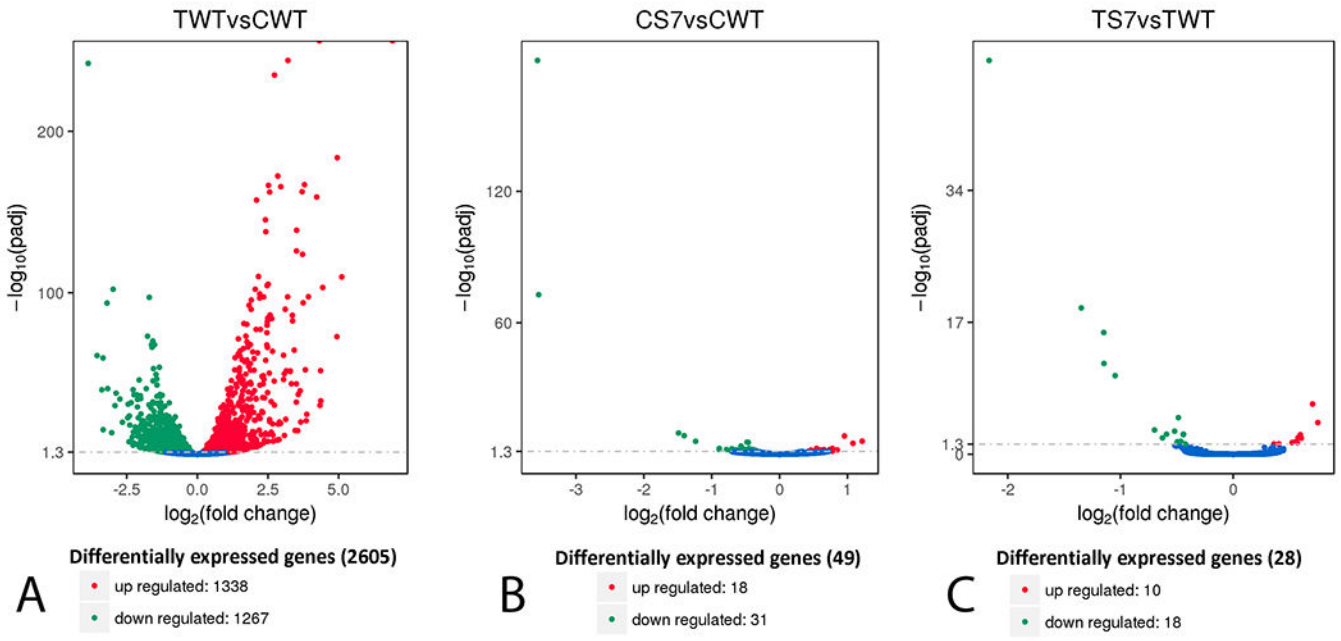

Figure 11: Effects of Smad7 loss on the transcriptional profile of TGF-β1-stimulated macrophages. A:

Volcano plot of RNA-seq data shows that TGF-β1 stimulation markedly altered the transcriptome of bone marrow macrophages (BMMs), inducing 1338 genes and downmodulating 1267 genes. B-C: Smad7 absence had modest effects on the macrophage transcriptome in both unstimulated and TGF-β-stimulated cells. Smad7 absence was associated with upregulation of 18 genes and downregulation of 31 genes in unstimulated BMMs (B). In TGF-β-stimulated cells, Smad7 loss was associated with induction of 10 genes and downmodulation of 18 genes (C). CWT, control wildtype; TWT, TGF-β-stimulated wildtype; CS7, control Smad7 KO; TS7, TGF-β-stimulated Smad7 KO.

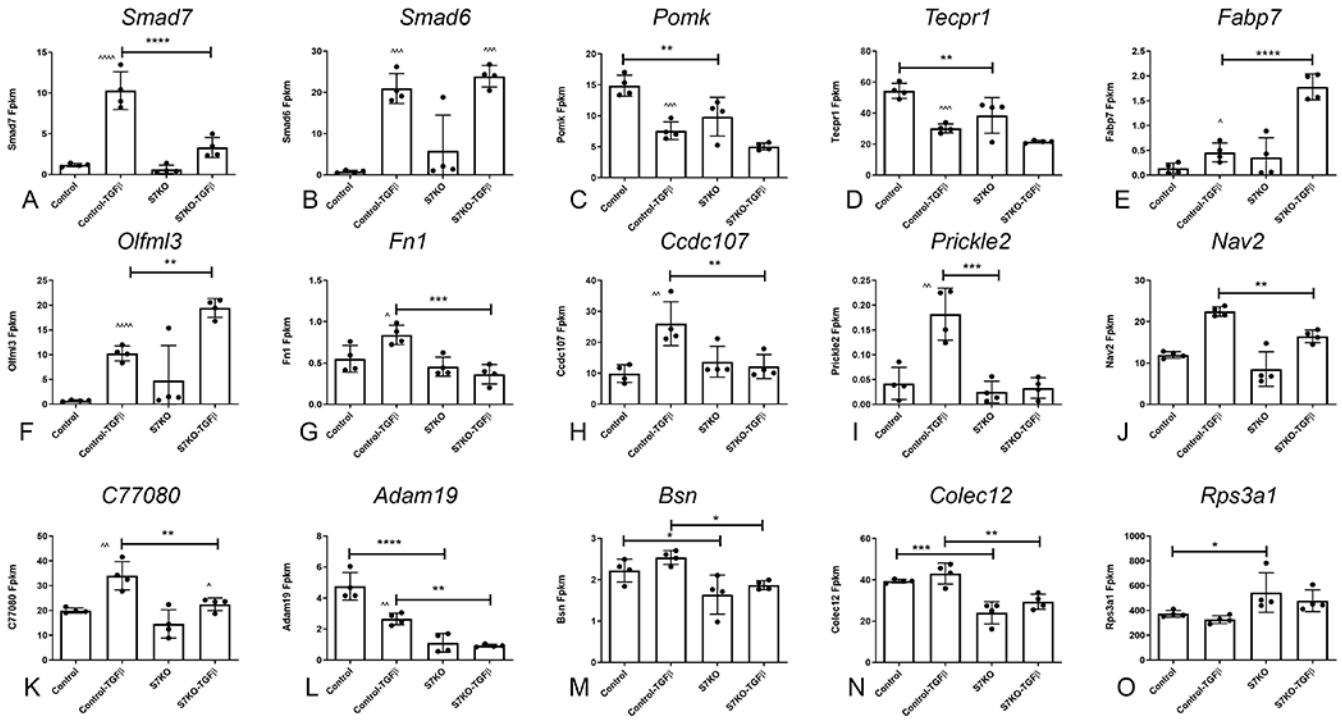

Figure 12: Effects of Smad7 loss on TGF-β1-stimulated gene expression in bone marrow macrophages (BMMs).

A: TGF-β1 induced *Smad7* expression was markedly reduced in Smad7 KO cells (S7KO). B: TGF-β1 stimulation induced comparable *Smad6* expression in both WT and Smad7 KO macrophages. The baseline transcription of *Pomk* (C), *Tecpr1* (D), *Adam19* (L), *Bsn* (M), and *Colec12* (N) was suppressed in S7KO macrophages. Smad7 absence markedly accentuated TGF-β1-induced expression of *Fabp7* (E) and *Olfm13* (F). In contrast, Smad7 loss attenuated TGF-β-induced expression of *Fn1* (G), *Ccdc107* (H), *Prickle2* (I), *Nav2* (J), *C77080* (K), *Adam19* (L), *Bsn* (M) and *Colec12* (N). (*p<0.05, **p<0.01, ***p<0.001; n=4/group).